Design, Analysis and Performance Evaluation of Indirect Solar Dryer

A Dissertation

Submitted in partial fulfillment of the requirement for the award of the degree
of
Master of Engineering
in
Renewable Energy

by

Tandin Jamtsho

Division of Energy and Building Design
Department of Energy Sciences

Electrical Engineering Department

Supervisor: Dr. Henrik Davidsson

Co-supervisor: Mr. Cheku Dorji

Examiner: Dr. Martin Andersson

October, 2023

Design, Analysis and Performance Evaluation of Indirect Solar Dryer

A Dissertation

Submitted in partial fulfillment of the requirement for the award
of the degree
of
Bachelors of Technology
in
Power Engineering
by
Dechen Om

Division of Energy and Building Design
Department of Energy Sciences

Electrical Engineering Department

Supervisor: Dr. Henrik Davidsson

Examiner: Dr. Martin Andersson

June, 2023

Acknowledgement

We want to express our sincere gratitude to everyone who played a vital role in the successful completion of our thesis. We are particularly thankful to the Linnaeus-Palme partnership organization for allowing us to pursue this research as exchange students in Sweden. We are deeply appreciative of Dr. Henrik Davidson, our supervisor, for his unwavering support and invaluable guidance throughout our thesis. Our time in Sweden was made much more manageable and enjoyable due to the assistance and kindness we received.

We are also grateful to our Examiner, Dr. Martin Andersson, for dedicating his valuable time to thoroughly evaluate our work and provide constructive criticism, which significantly contributed to improving our thesis. Special thanks to our professors in Bhutan, Dr. Tshewang Lhendup, and Mr. Cheku Dorji, for their constant support and guidance.

We want to acknowledge Mr. Christian Rissler for his kindness, hospitality, and significant contribution to our thesis. We are also thankful to Ms. Linnea Ekman for her cheerful company and guidance during our stay in Sweden. Our friends, family, and everyone whose names we couldn't mention also deserve our gratitude for their support.

The meticulous evaluation of our work, coupled with the valuable feedback and constructive criticism provided, has greatly enhanced the quality and advancement of our thesis. We truly appreciate the dedication and effort invested by all involved.

Candidate’s Declaration

I hereby certify that the work being presented in this Dissertation entitled **“Design, Analysis and Performance Evaluation of Indirect Solar Dryer”** in partial fulfillment of the requirement for the award of degree of Master of Engineering in Renewable Energy at College of Science and Technology, Royal University of Bhutan and submitted to the *Division of Energy and Building Design*, *Department of Energy Sciences, LTH, Lund University* is an authentic record of my work carried out during the period from January 2023 to October 2023 under the supervision and guidance of Dr. Henrik Davidsson, Lecturer (Lund University) and Mr. Cheku Dorji, Lecturer, College of Science and Technology.

The matter embodied in this dissertation has not been submitted by me for the award of any other degree.

Dated: October 2023
Place: College of Science and Technology

(**Tandin Jamtsho)**
Student Number at CST: 02220011
Student Identification at Lund university: ta8884ja

This is to certify that the above-mentioned statement made by the candidate is correct to the best of my knowledge.

(Dr. Henrik Davidsson)
Lecturer
Energy and Building Design
Building & Environmental Technology
Lund University
Sweden

(Mr. Cheku Dorji)
Lecturer
Department of Electrical Engineering
College of Science and Technology
Royal University of Bhutan
Bhutan

Candidate's Declaration

I hereby certify that the work being presented in this Dissertation entitled **"Design, Analysis and Performance Evaluation of Indirect Solar Dryer"** in partial fulfilment of the requirement for the award of the degree of Bachelor of Technology in Power Engineering at Jigme Namgyel Engineering College, Royal University of Bhutan and submitted to the *Division of Energy and Building Design, Department of Energy Sciences*, *LTH, Lund University* is an authentic record of my work carried out during the period from January 2023 to June 2023 under the supervision and guidance of Dr. Henrik Davidsson, Professor, Lund University.

The matter embodied in this dissertation has not been submitted by me for the award of any other degree.

Dated: June, 2023
Place: Jigme Namgyel Engineering College

(Dechen Om)
Student Number at JNEC: 05200005
Student Identification at Lund university: de6741om

This is to certify that the above-mentioned statement made by the candidate is correct to the best of our knowledge.

(Dr. Henrik Davidsson)
Lecturer
Energy and Building Design
Building & Environmental Technology
Lund University
Sweden

(Dr. Tshewang Lendrup)
President
Jigme Namgyel Engineering College
Royal University of Bhutan
Bhutan

Abstract

Food production is a critical component of global livelihoods and economic revenue. However, storing harvested food presents challenges in minimizing post-harvest losses. Among various methods, food drying has emerged as a popular technique for preserving food during off-seasons. The Solar Food project aims to design an affordable solar-powered food dryer that enhances the drying process and maintains the nutritional content of the food.

The study focuses on designing and evaluating an improved solar fruit dryer with a larger absorber area. It incorporates a low-density polyethene heat exchanger, a drying chamber, a heat storage system, and an air circulation fan. Various parameters, including drying rate, energy efficiency, and the quality of dried fruits, are analyzed to assess the dryer's performance. Results indicate that using a superior internal fan increases the drying rate of apples, and variations in drying rates are observed among differently positioned trays. Plastics prove to be efficient heat exchangers in the solar fruit dryer, achieving high efficiency with minimal flows.

The application of heat storage in the drying process initially absorbs energy and subsequently provides energy to the system after two hours of drying. The study suggests that employing better internal fans can reduce discrepancies in drying rates among different trays. The research contributes to the development of an improved solar fruit dryer by enhancing drying efficiency and minimizing post-harvest losses. These findings pave the way for more sustainable and effective food preservation methods, benefiting agricultural communities worldwide.

Table of Contents

1. Introduction

Dried fruits have been an integral part of human diets for millennia and have experienced a growing popularity. It demonstrates versatility in various culinary applications, such as being incorporated into baked goods, trail mixes, and salads. Its inclusion in a balanced diet contributes to energy levels, regulation of blood sugar, and promotion of digestive health (Jackson & White, 2020). Recognizing the substantial role of dried fruit in daily dietary intake is crucial due to the associated benefits it provides.

Solar drying, utilizing solar energy in fruit solar dryers to extract moisture, is a highly effective method for extending the shelf life of fruits. Implementing fruit solar dryers significantly reduces post-harvest losses and boosts farmers' income. These dryers are simple and efficient, consisting of a drying chamber, solar collector, and fan for air circulation. The solar collector harnesses sunlight to generate heat, dehydrating the fruits in the drying chamber, while the fan ensures uniform drying (Dobrev et al., 2018).

The utilization of solar dryers brings numerous benefits. It reduces reliance on fossil fuels and electricity, establishing an environmentally sustainable option. Solar drying preserves the natural qualities of fruits, including flavour, colour, and nutrient content, enhancing their nutritional value. These dryers are user-friendly and require minimal maintenance, making them suitable for rural and remote areas with limited access to electricity. Additionally, farmers can increase their income by producing dried fruits, which have a higher market value compared to fresh fruits. Embracing fruit solar dryers promotes sustainable agriculture and aids in mitigating post-harvest losses in line with the global shift toward renewable energy sources (Dobrev et al., 2018).

1.1. Project Background

This report was written as part of Solar Food: Reducing post-harvest losses through an improved solar drying project. This ongoing initiative between Lund University and the Royal University of Bhutan aims to enhance the quality of food and mitigate post-harvest losses in rural areas by implementing cost-effective solar-powered food dryers. Through conducting comprehensive experiments, the objective is to investigate the following research questions, forming the foundation of the inquiry and enabling to provide valuable insights into the optimization of solar food drying technologies and their potential impact on reducing post-harvest losses in rural areas:

- To what extent does the size of the absorber contribute to increasing the efficiency of the dryer?
- Is low-density polyethene a feasible option for use as a heat exchanger?
- Does removing heat storage affect the drying rate?
- What influence does the number of trays inside the dryer have on the drying rate?
- How does the internal flow of air circulation within the dryer impact its drying efficiency?

Addressing these research questions will provide valuable findings and contribute to our understanding of enhancing solar food drying methods, thereby aiding in the reduction of post-harvest losses in rural areas.

1.2. Project Introduction

In Bhutan, the lack of storage facilities and preservation technologies adapted to the prevailing conditions leads to high levels of post-harvest losses. Inadequate infrastructure hinders the effective storage and protection of harvested crops, leaving them vulnerable to pests, humidity, temperature fluctuations, and contamination (Wangmo & Dendup, 2021). Additionally, the absence of tailored preservation technologies further exacerbates the problem, as Bhutan lacks methods to extend shelf life or reduce spoilage. These combined factors result in significant losses, impacting food security, economic stability, and the livelihoods of farmers.

Drying food has been a crucial technique employed by food producers to ensure the preservation of post-harvest food and maintain a consistent food supply, even during off-seasons. Throughout history, people have relied on the simple method of sun drying, which involves placing food on mats under the sun. However, this method is not without its drawbacks. The direct exposure of food to sunlight during the drying process can lead to a deterioration in its nutritional value and cause colour changes, while the prolonged drying time creates an environment conducive to the growth of fungi and other microorganisms (Sharma et al., 2009). Open-sun drying methods further expose the food to contaminants like dust, airborne moulds and fungi, insects, rodents, and other animals, compromising its overall quality and safety. Moreover, the effectiveness of this traditional approach is limited in humid climates (Singh, 2015).

To overcome the limitations of sun drying, innovative designs and technologies have been developed, with solar food dryers emerging as a significant improvement upon the ancient method of food dehydration. Although solar dryers involve an initial investment, they offer numerous advantages. Firstly, they yield visually appealing, flavorful, and more nutritious foods, enhancing both their market value and nutritional content (Bala & Woods, 1994; Kilanko et al., 2019). Solar dryers are also faster, safer, and more efficient compared to traditional sun drying techniques. Specifically, an enclosed cabinet-style solar dryer can effectively produce high-quality dried foodstuffs even in humid climates, minimizing contamination risks. The shorter drying time in solar dryers reduces the likelihood of spoilage, while fruits retain a higher vitamin C content, ensuring better food quality (Gwala & Padmavati, 2015). Furthermore, as solar dryers generally require no additional fuel, they contribute to the conservation of non-renewable energy sources, making them an environmentally friendly method of food preservation (Singh, 2015).

2. Background

2.1. Solar Dryer in the Himalayan Regions

Agriculture in Himalayan regions has to consider lots of hurdles like the harsh climatic conditions, complex geological structures and irregular rainfalls. Consequently, the farmers in the Himalayan regions can produce food at only certain times of the year and consume the stored food for the other times of the year. With no proper food storage and preservation, like farmers in other countries, the farmers in the Himalayan region always opt for the drying of the food they produce and storing it for the off-season to survive. The open sun drying is the most common method one can find in the Himalayan regions to preserve the food. Though open sun drying is quite a fast and effective method to preserve food, the disadvantages are many, and one of the main problems is spoilage of the products due to weather conditions such as rain, wind and dust (Can, 2000). The hygiene is difficult to maintain, with contamination from the soil. Animals, insects and birds are also a source of contamination of microorganisms, and they also cause losses by eating the products if they get the chance.

2.2. Apple as the chosen fruit for the experiment

Apple is one of the very popular fruits consumed around the world. Apples are very commonly produced horticultural crops as well as cash crops in the Himalayan regions therefore, drying apples in solar dryers in the Himalayan regions can help in the preservation and storage of the apples with lower deteriorations in their nutrient contents. After that, the apple's firmness and flavour drop during long-term storage, which eventually causes a decrease in edible quality and commercial value. To preserve the nutrients in the apples and store them for a longer period, a solar dryer can be proven as one of the alternatives in doing so.

3. Solar Dryer

A solar dryer with a heat exchanger is an enhanced variant of a conventional solar dryer, incorporating a modified component to enhance its effectiveness (Kumar et al., 2017). By incorporating a heat exchanger along with a large solar collector, the dryer's efficiency is improved. The heat exchanger preheats the incoming air, minimizing the temperature disparity between the incoming and outgoing air streams. As a consequence, the drying process becomes more uniform and efficient, leading to the production of dried products of superior quality (Kumar et al., 2017).

The heated air from the collector is passed through a heat exchanger. The incoming cool air is preheated and then passed to the drying chamber and a fan circulates the hot air inside the chamber, speeding up the drying process. The food is placed on the trays inside the drying chamber, and the hot air dries the food by evaporating the moisture content. As the moisture evaporates, it is carried away by the hot air, which exits the chamber through a chamber outlet. The solar dryer for this project typically consists of main components like a solar collector, a drying chamber, fans (internal and external), heat storage, and a heat exchanger.

3.1. Solar collector

A solar collector also known as an absorber is the part of the dryer that absorbs the sun's rays and converts them into heat. Initially, the absorber was usually made of a dark-coloured material that has high thermal conductivity, such as aluminium, copper, or steel. However, some less conventional materials like plastic could also be used with the same impact for the solar collector. The absorber used for the dryer measures around one square meter of a metal sheet painted black on both sides and covered with glass which helps to absorb the sun's rays and minimize the amount of heat that is lost through radiation.

Although some research studies suggest that smaller gaps result in more efficient heat transfer, considering the thermal expansion of the fluid (Yilmaz & Hires, 2014; Chowdhury et al., 2012), a narrow gap of 1 cm on both sides of the absorber was used as shown in *Figure 3-1*.

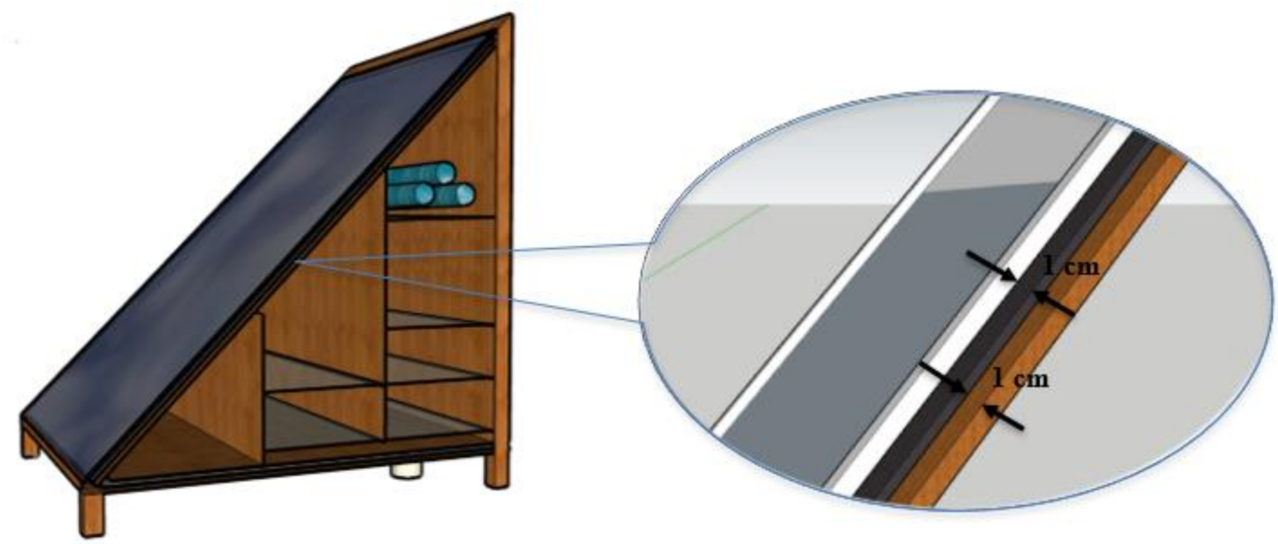

Figure 3-1: A narrow gap of 1 cm was used between the absorber and the glass as well as from the plywood below.

This choice allows us to maximize the surface area available for heat transfer to the flowing air while it poses less difficulty in building it. Additionally, the absorber was positioned at a 45° inclination from the ground to ensure that solar irradiation strikes the collector surface perpendicularly. The efficiency of the absorber was calculated using the formula:

$$Absorber\ efficiency = \frac{Energy\ absorbed\ by\ the\ fluid}{Solar\ irradiance\ incident\ on\ the\ absorber}$$

$$\eta = \frac{f_m\ c_p\ \ \Delta T}{I\ \ A}$$

(3.1)

where f_m is the mass flow, c_p is the specific heat of the air, ΔT the temperature difference, I is the intensity of solar radiation and A the surface area of the absorber. The mass flow is given by:

$$F_m = V_{air} \times\ A_{cross}\ \times \rho_{air}$$

(3.2)

Where, V_{air} is the velocity of the airflow, A_{cross} the cross-sectional area of the flow and ρ_{air} density of the air.

3.2. Heat storage

In a solar dryer, heat storage is an important aspect that helps to maintain a consistent drying temperature and ensures that the drying process is effective. Heat storage in a solar dryer can be achieved through the use of materials with high thermal mass, such as bricks, concrete, or stones. Heat storage is used for storing heat energy for a long period, and releasing the heat steadily, which helps to maintain a consistent temperature inside the solar dryer.

In this dryer, the water was used as the heat sink to maintain the constant temperature in the dryer. Three bottles of 1.5 litres each were filled with water and placed right before the entrance of the air coming inside the drying chamber after being heated by the absorber. These filled bottles supposedly act as heat storage for the dryer and try to maintain a constant temperature in the dryer throughout the drying period.

3.3. Heat Exchanger

The dryer's heat exchanger operates on a counter-flow system, where the flow direction on one side is opposite to the other side, enabling optimal heat transfer. Theoretically, it's possible to transfer all the heat energy from the hot side to the cold side using this approach, but in reality, there are always some heat losses, which reduces its efficiency. One of the main objectives of this project was to make an efficient dryer but also a cost-effective one at the same time. So, one best way to reduce cost was replacing the whole heat exchanger with an inexpensive plastic material.

The equation for heat exchanger efficiency on the cold side, assuming equal mass flow on both sides, is the following (Cengel 2002):

$$\eta_{cold} = \frac{T_{out\_cold} - T_{in\_cold}}{T_{in\_hot} - T_{in\_cold}} \tag{3.3}$$

The efficiency on the hot side is given by:

$$\eta_{hot} = \frac{T_{in\_out} - T_{out\_hot}}{T_{in\_hot} - T_{in\_cold}} \tag{3.4}$$

The heat exchanger can also serve as a means to detect potential leakage problems. When there is no leakage, the principle of mass conservation dictates that an equal amount of air will flow on both sides of the heat exchanger. The temperature differences observed on both sides of the heat exchanger should be identical due to the conservation of energy if there is no condensation. However, in the presence of leakage, the mass flow on the hot side will decrease while the conservation of energy remains true. This alteration in mass flow will lead to a more pronounced temperature variation on the hot side since the outflow from the solar dryer will be reduced compared to the inflow it receives. Consequently, by continuously comparing the temperature differences on both sides, valuable insights into the system's airtightness can be obtained, offering transparency and enabling timely identification of any leakage issues.

3.4. Drying chamber

The dryer has a drying chamber that is separated into two sections, chamber 1 and chamber 2. Chamber 1 has three trays, while Chamber 2 has two trays specifically designed for drying apples. *Figure 3-2* shows the schematic layout of the dryer with placement of the trays

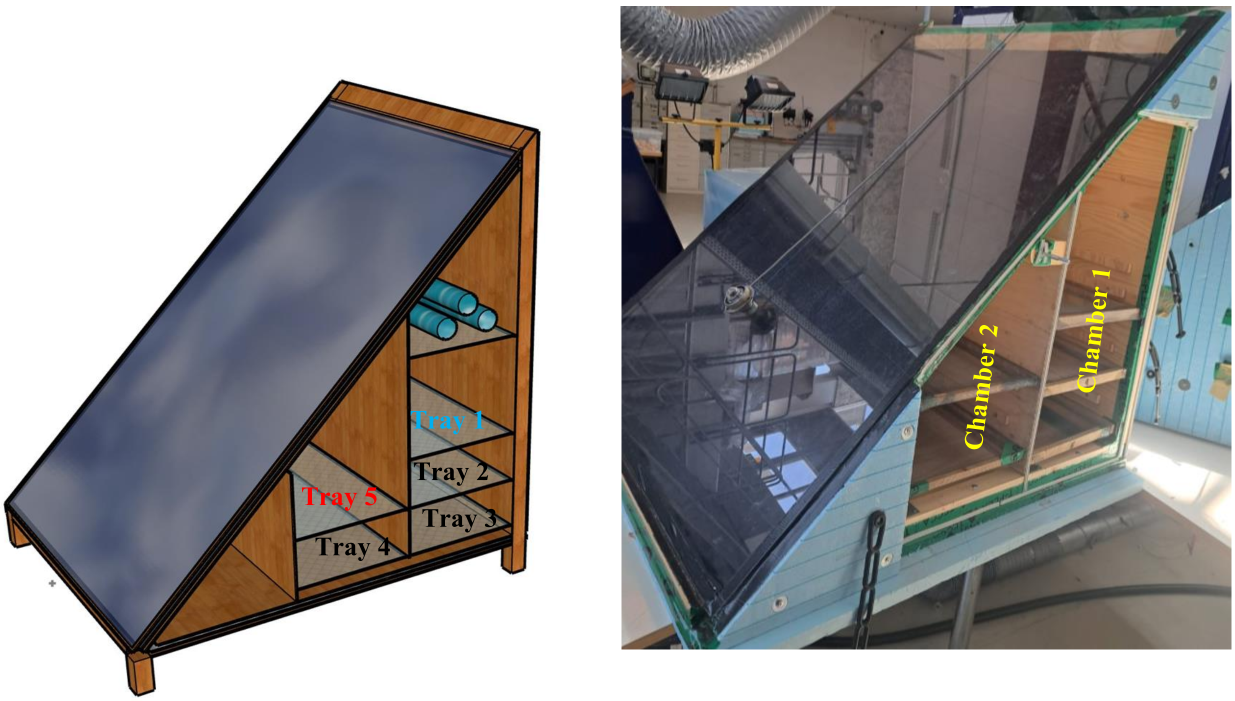

Figure 3-2: The positioning of the trays inside the drying chamber showing the best drying rate tray (blue) and least dying rate tray (red).

3.5. Internal and External Fans

The dryer is equipped with two fans: an external 12 V DC fan located at the base of the dryer just before the entrance of the heat exchanger, and an internal fan with the same rating positioned between the two drying chambers as mentioned earlier. The purpose of the external fan is to control the airflow into the dryer, and its speed can be adjusted by regulating the voltage from an external power source. On the other hand, the internal fan operates at a consistent voltage to ensure a steady airflow within the drying chambers, preventing the accumulation of hot air in a single area.

3.6. Airflow inside the solar dryer

Figure 3-3 illustrates the airflow in the solar dryer. The process begins with an external fan which draws in air from the surroundings through the inlet pipe as shown in *Figure 3-4*. This inlet airflow is represented by the blue arrow in the figure. The air is then directed through the lower section of the heat exchanger before entering the absorber from both sides.

Once within the absorber unit, the air experiences a rise in temperature before proceeding into the drying chamber. Inside this chamber at section B, the air comes into contact with the heat storage material. Continuing along its path, the air moves downwards through the initial three trays, following the arrangement illustrated in

Figure 3-3. Ultimately, it rises into the subsequent section. To guarantee even convection across the drying trays, an internal fan circulates the air within the compartment at section C. The swift air movement leads to uniform conditions throughout the drying chamber, ensuring an equal drying rate for all trays. Moreover, the increased air speed also amplifies the transfer of heat and moisture to and from the apple slices.

Finally, the air exits the chamber, being expelled through the hot side of the heat exchanger. This completes the cycle of air circulation within the solar dryer. The airflow mechanism is designed to facilitate efficient heat transfer, effective drying, and better convection throughout the system, promoting optimal drying conditions for the samples being dried.

Figure 3-3: The airflow paths inside the dryer with the air flowing in shown by the blue arrow and the air out of the dryer shown by the brown arrow.

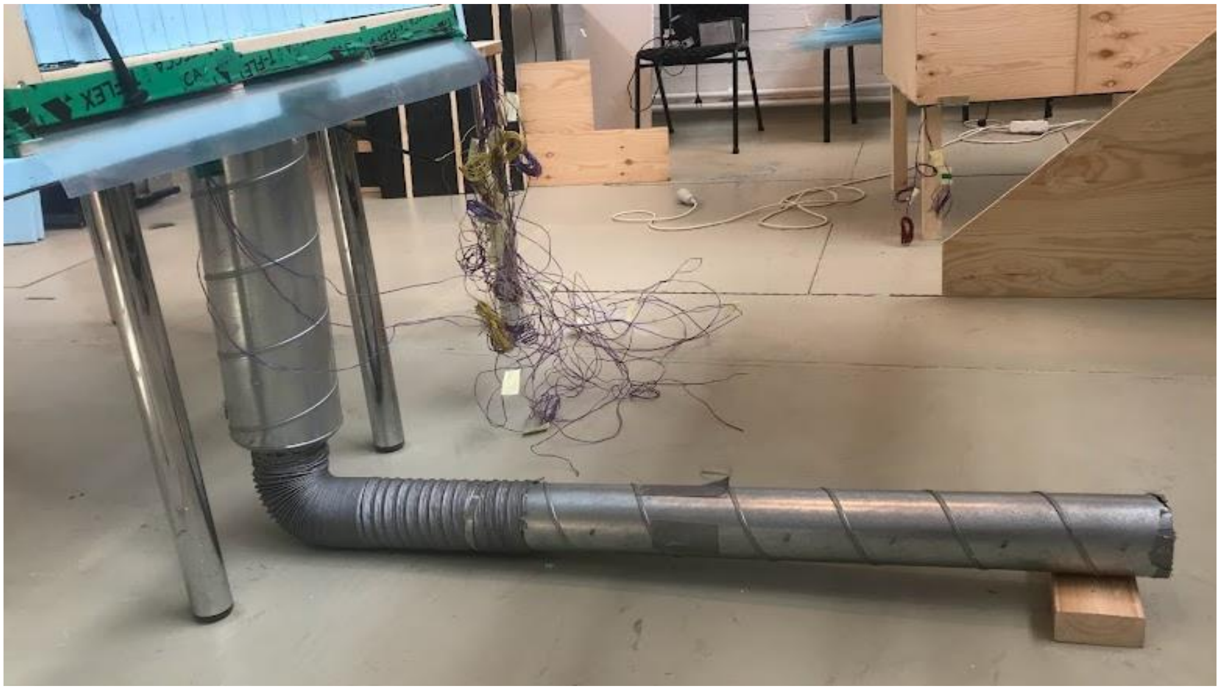

Figure 3-4: The inlet pipe through which the cold outer air is sucked by an external fan fixed at the start of the bigger diameter pipe.

3.7. Density of the air

The air density at standard conditions of 1 atmosphere and 25 °C is approximately 1.17 kg/m³ (Engineering Toolbox, 2003). However, when considering the specific altitude of the dryer, which was roughly 47 meters above sea level, the air density and pressure differ from those at sea level (Elevation of Lund, Floodmap.net, n.d.). To determine the air density at this altitude, the first step is to find the air pressure using the equation:

$$p = p_{atm}(1 - 2.25577 \times 10^{-5} h)^{5.25588} \tag{3.5}$$

Here, h represents the height in meters, and patm is the atmospheric pressure at sea level, assumed to be 1 atm. By applying this equation, it can be calculated that the atmospheric pressure is 0.994 mbar at an altitude of 47 meters.

To determine the density, the ideal gas law can be applied:

$$PV = RT \tag{3.6}$$

where P is pressure, P is volume, R is the gas constant, and T is temperature. By rewriting the volume as weight divided by density, the density solution can be obtained:

$$\rho = \frac{P_m}{RT} \tag{3.7}$$

Dividing both sides of the equation by the corresponding equation for standard density and pressure at sea level, with the same mass and temperature, the following equation is derived:

$$\frac{\rho}{\rho_{atm}} = \frac{P}{P_{atm}} \tag{3.8}$$

From this, it can be determined that the density of air at an altitude of 47 meters is approximately 1.163 kg/m^3, which has been utilized in heat flux equations to ensure accurate energy and efficiency calculations.

4. Methodology

4.1. Preparation of sensory equipment

The various types of sensors used in the whole study are given below with their preparation and calibration.

4.1.1. Thermocouples

A total of 23 thermocouples of type J were prepared with appropriate lengths to facilitate temperature measurements. Approximately 5 mm of the protective covering was removed from the end, and the exposed tips were soldered together. These thermocouples were subsequently connected to a Campbell Scientific Multiplexer 16/32, which was in turn linked to a Campbell Scientific CR1000 Data Logger. The data collected from the thermocouples could then be monitored and recorded using PC400 software via a USB connection to a computer.

Before commencing the data collection process, the accuracy of the thermocouples in measuring temperature was verified. This was accomplished through two setups. Firstly, hot boiling water was utilized to determine if the measured temperature corresponded closely to the boiling point of water. Secondly, ice-cold water was employed to confirm that the thermocouples accurately recorded the lowest temperatures. The results of these tests indicated that the readings obtained from the thermocouples fell within the expected range, validating their temperature-sensing capabilities.

The sensors were employed to monitor and record temperature measurements across various sections of the dryer. *Figure 4-1* illustrates the placement of three thermocouples at each designated location, specifically at the rear, back, middle, and front positions. However, in the case of the drying chamber, a slightly different approach was taken. To ensure accurate temperature readings of the heated air from the absorber outlet, the sensors were strategically positioned, with three sensors in the first chamber and two sensors in the second chamber. Care was taken during the sensor placement to shield them from direct radiation emitted by the lamp, as their purpose was to solely measure the temperature of the heated air rather than external influences.

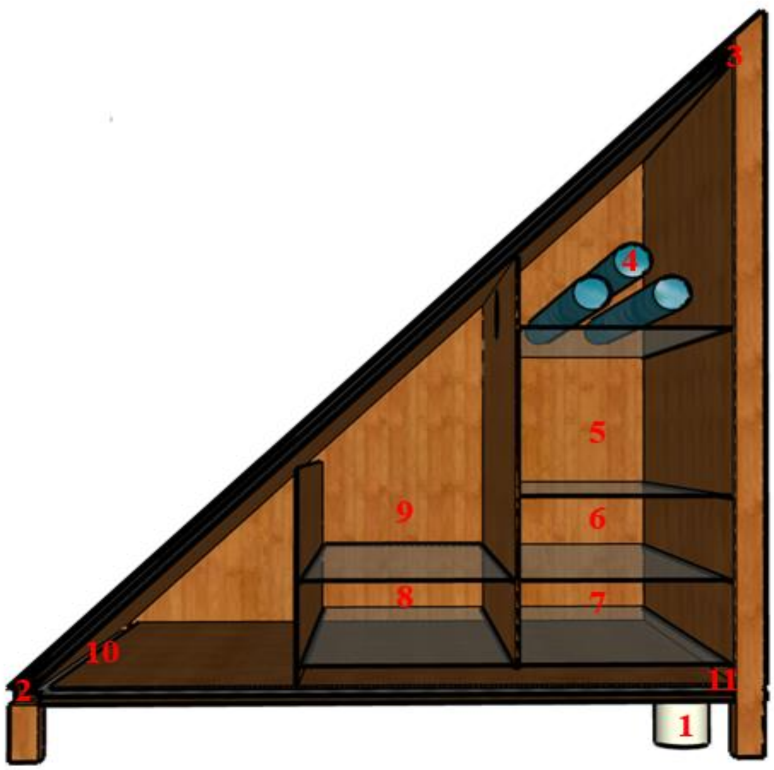

Figure 4-1: Placements of the thermocouples inside the dryer. The number corresponds to the 3 sensors placed except for the numbers 5, 6, 7, 8, and 9 where only one sensor is placed. The numbering of the sensors at different parts represents 1. Dryer inlet, 2. Absorber inlet, 3. Absorber outlet, 4. Heat storage, 5, 6, 7. Chamber I temperature, 8, 9. Chamber II temperature, 10. Drying chamber outlet, 11. Dryer outlet.

4.1.2. Pyranometer

The measurement of irradiation is conducted using a CM 5 pyranometer, which has a precision of ± 5 W/m². This instrument is specifically engineered to gauge the irradiance on a flat surface, taking into account both the direct radiation and the diffuse radiation it receives (Kipp & Zonen, n.d.). It has a sensitivity of 16.9 μV/W/m² and it was directly connected to the Campbell Scientific CR1000 Data Logger. The recorded solar irradiation from the pyranometer was subsequently cross-verified using a handheld Frederiksen's Hand Pyranometer 4890.20 (Cm, n.d.)

4.1.3. Relative humidity data logger

The relative humidity inside the dryer was monitored using the Extech SD800 Temperature/Humidity/CO_2 Data Logger with a resolution of ± 4 % RH at intervals of 30 seconds. Since only one data logger was available, it was positioned in the tray with the optimal drying rate to observe the variations in relative humidity with the drying rate and the temperature in that specific location inside the dryer (Min & Max, n.d.).

4.2. Air flow measurements

The airflow measurement techniques utilized in this study were derived from the work of (Johansson et al., 1999). According to their method, when dealing with a circular canal, the flow should be measured at a distance of at least two times the canal diameter from the external fan and five times the diameter of the pipe from the air intake these requirements were comfortably surpassed. The airflow was assessed using a Testo 416 vane anemometer, which has a resolution of 0.1 m/s. The anemometer probe, with a length of 890 mm, was positioned at a depth of 29 mm and 71 mm, with one measurement taken from the top and one from the side. To accommodate the anemometer probe, a hole was drilled at the designated locations. It should be noted that the airflow within the pipe is highest at the centre and slower at the walls, creating a gradient of flow between them. (Johansson et al., 1999) suggest that for a 100 mm diameter pipe, the flow at distances of 29 mm and 71 mm represents the average flow throughout the pipe. Therefore, the average of these four flow measurements is used to determine the airflow entering the dryer.

Furthermore, a different anemometer, specifically the Swema Air 30 thermal anemometer, was employed to estimate the internal airflow within the dryer. This particular anemometer offers a significantly improved resolution of 0.01 m/s. The purpose of measuring the internal airflow was to investigate the potential factors contributing to the disparity in drying rates observed between the trays positioned in two distinct chambers of the dryer.

4.3. Sample preparation

To collect data using the 5 original trays, 2.5 *kg* of apples were used, distributing 0.5 *kg* per tray. To initiate the experiment, the six apples were randomly selected and weighed using a kitchen scale with a precision of 1 *g*. Additionally, the volume of these apples was determined by utilizing a beaker and the water displacement method. The recorded weight and volume of the sample for later use in calculating the bulk density of the apples employed in the experiment. The formula used for this calculation is as follows:

$$\rho = \frac{m}{V} \tag{4.1}$$

where ρ is the density, m is the mass and V *is* the volume. Equation *(4.1)* provides the bulk density of the sampled apples in kilogram per cubic meter (kg/m^3). This bulk density value is subsequently utilized to determine the surface area of the apple that is exposed to the flow of air as given by the following formula:

$$A_s = \left(\frac{M/\rho}{t}\right) \times 2 \tag{4.2}$$

where A is the surface area of the apple exposed to the flow, M is the mass of the apple, ρ the density of the apple and t is the thickness of the slice of the apple.

As shown in equation *(4.2)*, it is important to note that the mentioned area calculation does not consider the thin curved surface area of the apple. This omission is due to the narrowness of the apple slices, which would complicate the calculations and is unlikely to have a significant impact on the final result.

Fresh apples were cut into pieces using a mandoline slicer. A small group of slices, selected at random, were stacked together and their combined thickness was measured. This measurement was then divided by the number of slices to determine the average thickness t of each slice in the sample. Following that, the apple slices were carefully allocated to individual trays within the dryer as shown in *Figure 4-2*, ensuring minimal overlap between them, to facilitate the experiment.

Figure 4-2: Apple slices on a tray placed inside the dryer with minimal overlapping between the slices.

4.4. Drying rate calculation

The drying rate was one of the important factors considered in this report. It shows how many grams of water inside the sample have dried over a specific time per unit area. It is given by the formula:

$$DR = \frac{m_{init} - m_{final}}{t \times A_s} \tag{4.3}$$

Where *DR* is the drying rate, m_{init} is the initial mass of the apple, m_{final} is the final mass of the apple, t is the time and A_s is the total surface area of the apple.

4.5. Data collections

The drying process and data collection took place at Lund University in Sweden in a laboratory setting. To replicate solar radiation, a solar lamp consisting of seven powerful bulbs, each rated at 2500 *W*, was used. The experiments spanned approximately 20 working days, during which different parameters were adjusted every three days. Initially, the apples were subjected to a continuous drying period of 8 hours, with varying airflows of 10 l/s, 15 l/s, and 20 l/s. However, it was observed that the apples dried much faster than expected. To determine and verify the apple's constant drying rate, subsequent experiments were conducted, involving hourly weight measurements over an eight-hour duration. Following this, the experimental setups were executed and tested as outlined below.

4.5.1. Control experiment (Hourly measurements of the individual tray and changing the flows)

Building upon the insights gained from the initial tests with different flows, the experiments proceeded to gather data for three different air flows: 20 l/s, 15 l/s, and 10 l/s. To track the drying progress, the weight of the apple in each tray was measured on an hourly basis over eight hours. The primary objective of this data collection was to identify the approximate time at which all the trays exhibited similar drying rates. At each hourly interval, the dryer was carefully opened and the weight of the apples in each tray was recorded, aiming to detect any variations in drying rates among them.

The core focus of this experiment revolved around determining the consistency of the drying rate throughout the data collection period. By analyzing the results obtained from this control experiment, the assessment of whether the drying rate maintained a linear progression was made. This initial linear trend provided valuable insights into the behaviour of the drying process, offering a foundation for further analysis and experimentation on the dryer.

4.5.2. Drying for three hours straight with 20 l/s, 15 l/s and 10 l/s.

The initial findings from the experiment yielded valuable insights, revealing that the apples achieved the desired level of dryness in approximately 3 hours. This discovery informed the subsequent design of the data collection phase, which was specifically structured to cover a 3-hour duration which made it easier for comparison and analysis of different experiments.

In contrast to the previous experiment, where the dryer was periodically opened and the apples were weighed hourly, a different approach was adopted for this specific experiment. Here, the dryer operated continuously for the entire 3-hour duration without any interruptions for weighing purposes. This continuous operation allowed for a more uninterrupted drying process, eliminating potential disturbances that could affect the accuracy of the drying rate assessment.

Upon the conclusion of the 3-hour experiment, the individual trays of apples were weighed, and the total weight of the dried apples was determined. This collective information was then utilized to calculate the overall drying rate achieved during the 3 hours. Simultaneously, the drying rate for each tray was also calculated, considering the varying positions of the trays within the dryer. The purpose of this comparison was to identify any variations in the drying rate across different sections of the dryer and identify the specific area that exhibited the highest drying rate. By analyzing the drying rates in different parts of the dryer, a comprehensive understanding of the drying process's spatial distribution was obtained.

4.5.3. Open air drying

In order to compare the efficacy of open-air drying with that of using a solar dryer, a comparative experiment was conducted using apple samples prepared identically. The apples were sliced to the same thickness, and they were sourced from the same batch, ensuring consistent characteristics such as size and moisture content. One tray of apples was directly placed under the irradiation from the lap on a flat surface. Additionally, another tray was placed in the shade, away from any artificial solar radiation. It is important to note that this experiment was conducted in a laboratory setting, and thus does not fully simulate real-world drying conditions, including factors such as wind and other weather elements. Furthermore, the quantity of apples used in each tray for this experiment was reduced to approximately 250 grams, which is half of the quantity used in the trays for the solar dryer experiment. The weight of the apple samples was measured every hour for 8 hours, enabling us to calculate the drying rate after each hour and draw comparisons between the different drying methods.

By conducting this comparative experiment, the differences in the drying rates and efficiency between open-air drying and the utilization of a solar dryer were to be tested. The tray dried under direct solar irradiation represented the scenario where the sun's energy was harnessed for the drying process, albeit without the specific angle of inclination as seen in the absorber of the solar dryer. On the other hand, the tray dried in the shade provided a baseline for open-air drying, devoid of any additional solar radiation. Despite the limitations of the laboratory environment, this experiment provided insights into the contrasting effects of these two drying methods.

4.5.4. Drying for 3 hours with a bigger internal fan

In order to explore the potential influence of an upgraded internal fan on the drying rate of the system, the existing smaller internal fan which measured 120 mm by 120 mm was replaced by a larger internal fan boasting a swept area of 140 mm by 140 mm. The hypothesis assumed that employing a larger internal fan would enhance the airflow within the dryer. It was believed that this augmentation in airflow would play a vital role in expediting the circulation and elimination of air-carrying evaporated water vapour from the fruit.

To accurately evaluate the effect of the larger internal fan, several parameters throughout the experiment were closely monitored. These included the temperature and humidity levels inside the dryer, and the overall drying efficiency. By comparing the data collected from this experiment with the results obtained from the use of the smaller internal fan in previous trials, we aimed to identify any significant improvements in the drying rate, as well as assess the overall effectiveness of the upgraded fan in enhancing the system's performance.

4.5.5. Drying with 4 more additional trays to 5 original trays with smaller and bigger internal fans.

In order to replicate real-world scenarios more accurately, an additional 4 drying trays to the existing 5 trays were added, resulting in a total of 9 trays. This adjustment allowed us to simulate a situation where a farmer would utilize the dryer on a larger scale. The experiments aimed to simulate the actual environment in which farmers would use solar dryers by adding more trays.

The first part of the experiment focused on using the smaller internal fan, as it had previously demonstrated the best drying rate for the dryer with a flow of 20 l/s, the drying performance of the nine trays under these conditions was tested. By employing the smaller internal fan, the baseline for comparison was established and identification of any disparities in the drying rates among the trays within the dryer was studied.

For the second part of the experiment, the smaller internal fan was replaced by a larger and more powerful alternative. With this upgraded internal fan, it was aimed to investigate whether its improved capabilities could minimize the variation in drying rates observed in the previous experiment. Running the experiment for 3 hours, utilizing a flow of 20 l/s, the impact of the enhanced fan on reducing the differences in drying rates among the trays within the dryer was found.

Based on the observations from the earlier experiment, a hypothesis was made that incorporating better and stronger internal fans would effectively decrease the disparity in drying rates among the trays. By upgrading to a larger fan, the improved airflow and circulation within the dryer would lead to a more consistent drying process. This hypothesis formed the basis for the decision to introduce the larger fan and investigate its potential to minimize the discrepancies in drying rates among the various trays.

4.5.6. Drying without heat storage

Investigating the impact of heat storage on the drying mechanism, an 8-hour experiment was conducted under constant solar irradiation using the smaller internal fan and the original 5 trays. Since the radiation remained consistent throughout the experiment, the heat storage system initially absorbed a significant portion of the energy that could have been used for drying the samples.

The drying process without heat storage was examined by recording the weight of each tray hourly. This allowed for an analysis of drying rates and various aspects of the dryer’s functioning, providing insights into how the absence of heat storage affected the drying rate and overall operation. Comparing these observations with the baseline or control experiment revealed distinctions in drying rates and the general behaviour of the dryer, offering valuable insights into the significance of heat storage and its role in enhancing the drying process.

5. Results

5.1. Constant drying rate with hourly measurements

In *Figure 5-1*, the weight of the apple slices is plotted against drying time, demonstrating results for three distinct air flows: 10 l/s in red, 20 l/s in blue, and 15 l/s in yellow trendline. The graph illustrates that increased airflow corresponds to a higher rate of drying. Overall, all three trend lines indicate that the drying process follows a consistent and predictable pattern for each flow. The close alignment of the data points with the trendlines suggests a strong linear correlation between drying time and apple weight. The findings suggest that the drying process at each flow can be effectively represented and understood through linear relationships between the drying time and the weight of the apples.

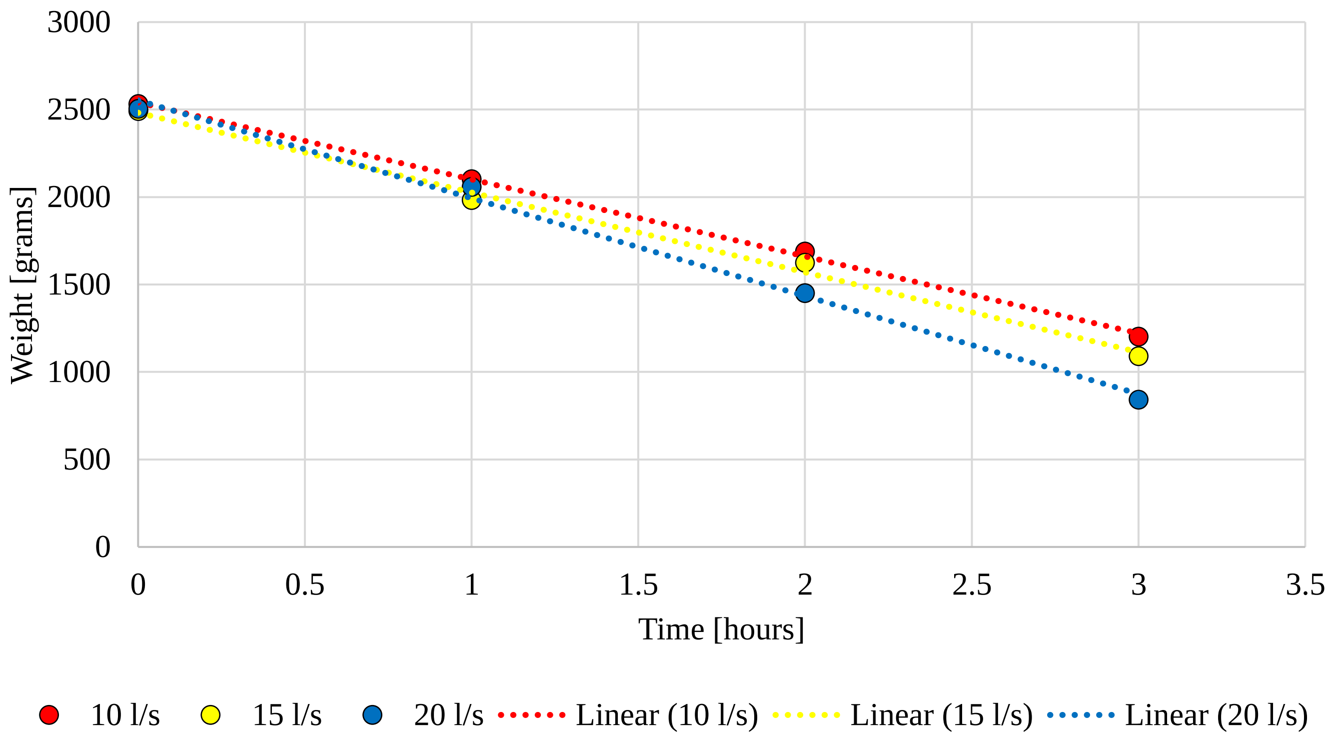

*Figure 5-1:*Weight of apple over time for three separate experiments, one with a flow of 10 l/s (red) and one with 15 l/s (yellow) and 20 l/s (blue).

5.2. General characteristics of the dryer

5.2.1. Heat exchanger

The trend shown in *Figure 5-2* indicates the overall heat exchanger efficiency with airflows. The efficiency of the heat exchanger decreases as airflow rates increase, following a second-degree polynomial pattern with an R^2-value of nearly 0.9. The most efficient point was observed at 2 l/s, reaching a high of 68%. However, it's important to note that the difference in efficiency between airflow rates of 10 l/s and 15 l/s is minimal. This implies that within this specific range, changes in airflow have a relatively minor impact on heat exchange effectiveness. While the decrease in efficiency shows a linear pattern with increasing airflow rates, it's crucial to consider that the trend in the graph results from a combination of various types of experiments.

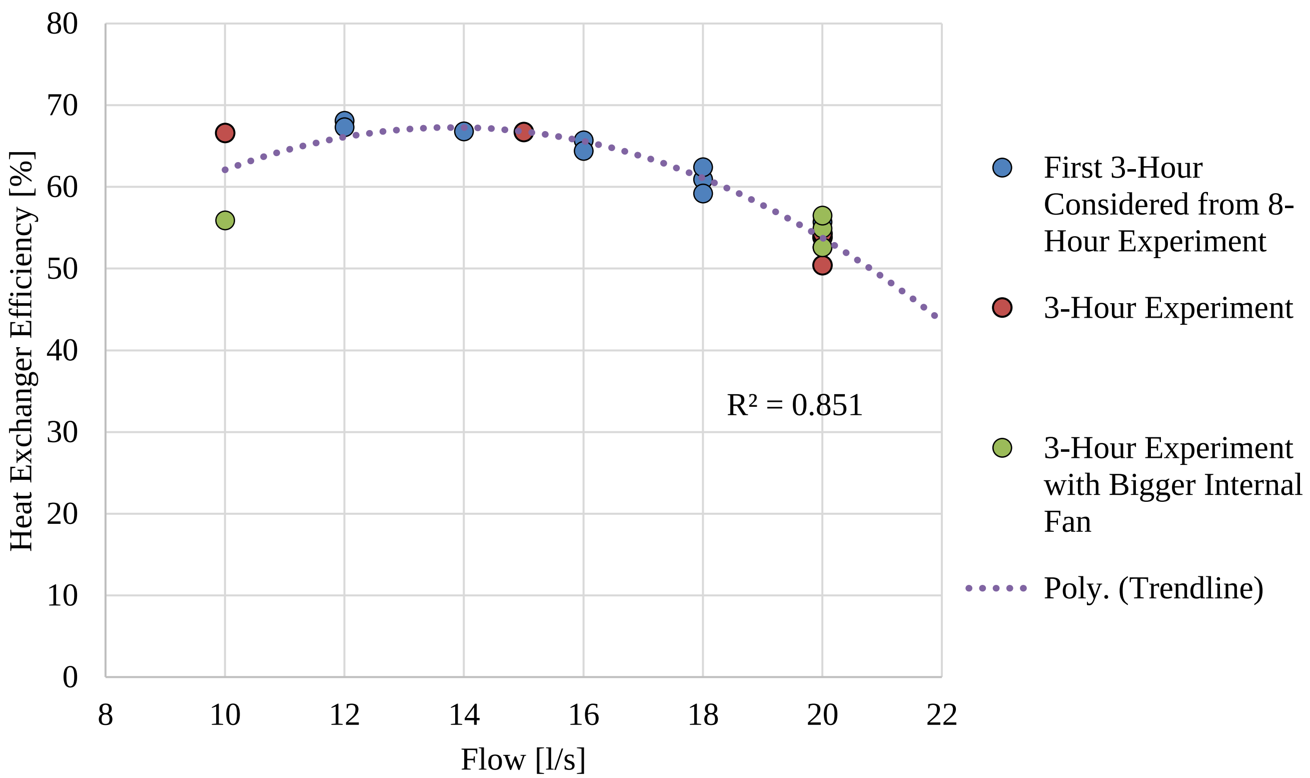

Figure 5-2: The average efficiency of the heat exchanger plotted over flow.

The heat exchanger's efficiency on the cold side, as well as the temperature difference on the cold side plotted against drying time, specifically for the flow of 20 l/s, is presented in *Figure 5-3*. The grey line in the graph represents the ratio between the temperature difference on the cold side and the temperature difference on the hot side, which consistently aligns closely with unity. This alignment indicates that there is minimal leakage occurring within the dryer, as the ratio remains consistent throughout the drying process. This suggests that the heat exchanger is effectively containing and transferring heat without significant losses, resulting in efficient operation and reduced energy wastage.

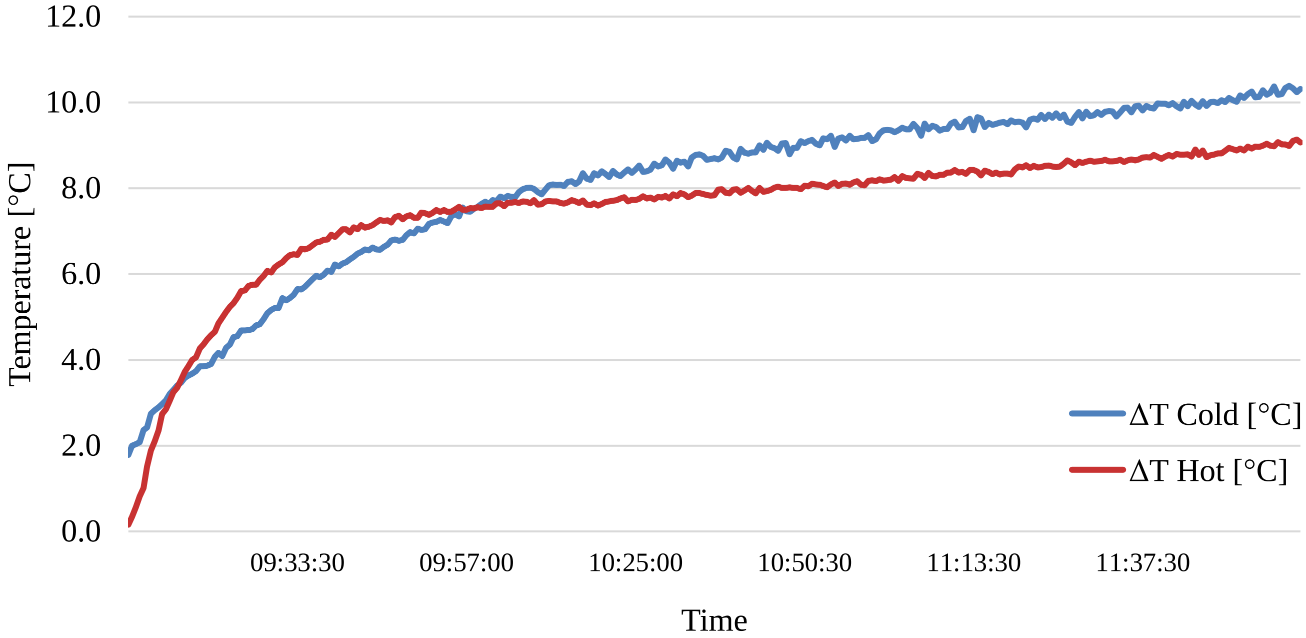

Figure 5-3: The temperature difference observed on the cold side is depicted by the blue line, while the red line represents the temperature difference on the hot side for 20 l/s on 23rd May.

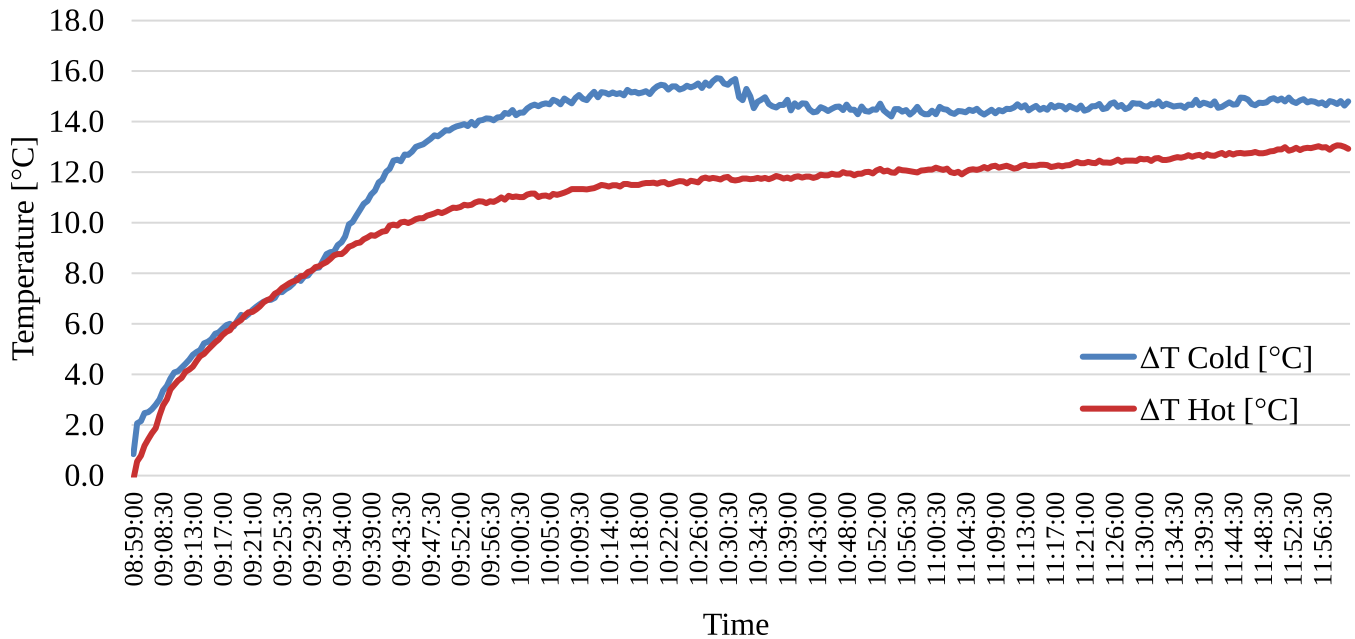

Figure 5-4: The temperature difference observed on the cold side is depicted by the blue line, while the red line represents the temperature difference on the hot side for 10 l/s on 24th May.

The experimental results depicted in *Figure 5-3* and *Figure 5-4* reveal an interesting phenomenon where the temperature difference on the cold side exceeds that on the hot side contrary to the flow of heat to the cold side from the hot side. Several factors contribute to this observation. One possibility could be the proximity of the hot side of the heat exchanger to the drying chamber, separated only by a 0.4 cm cardboard without insulation. This arrangement might result in the conduction of heat from the drying chamber into the hot side, reducing the temperature difference on that side and making the temperature difference on the cold side appear greater.

Insufficient insulation or poor thermal conductivity on the cold side, resulting in heat loss and a greater temperature drop could be another reason. Flow restrictions or imbalances within the heat exchanger can affect heat transfer efficiency, causing uneven temperature distribution. Measurement errors may also contribute, where sensor placement inaccuracies can affect the measured temperatures. Shifting outlet temperature sensors due to the expansion of low-density polyethene and contact with thermocouples could have introduced these errors. Additionally, condensation on the hot side has the potential to decrease the temperature difference, as the heat released during phase change transfers thermal energy to the surroundings.

Considering these factors, it is plausible to explain the unexpected temperature differences observed in the experiment. However, further analysis and investigation are required to precisely determine the underlying mechanisms and optimize heat transfer efficiency in the solar dryer's heat exchanger system.

5.2.2. Absorber

The data presented in *Figure 5-5* indicates that the efficiency of the dryer's absorber, unlike the heat exchanger, increases with the flow. The dryer achieved its highest absorber efficiency at 54.5% with an airflow of 20 l/s during a 3-hour experiment. While the trendline shows an increase from lower flows, it remains uncertain how the absorber will perform at airflow rates higher than 20 l/s based on these experiments. Overall, these results indicate that as airflow within the dryer increases, the absorber becomes more effective at capturing and utilizing solar energy for the drying process.

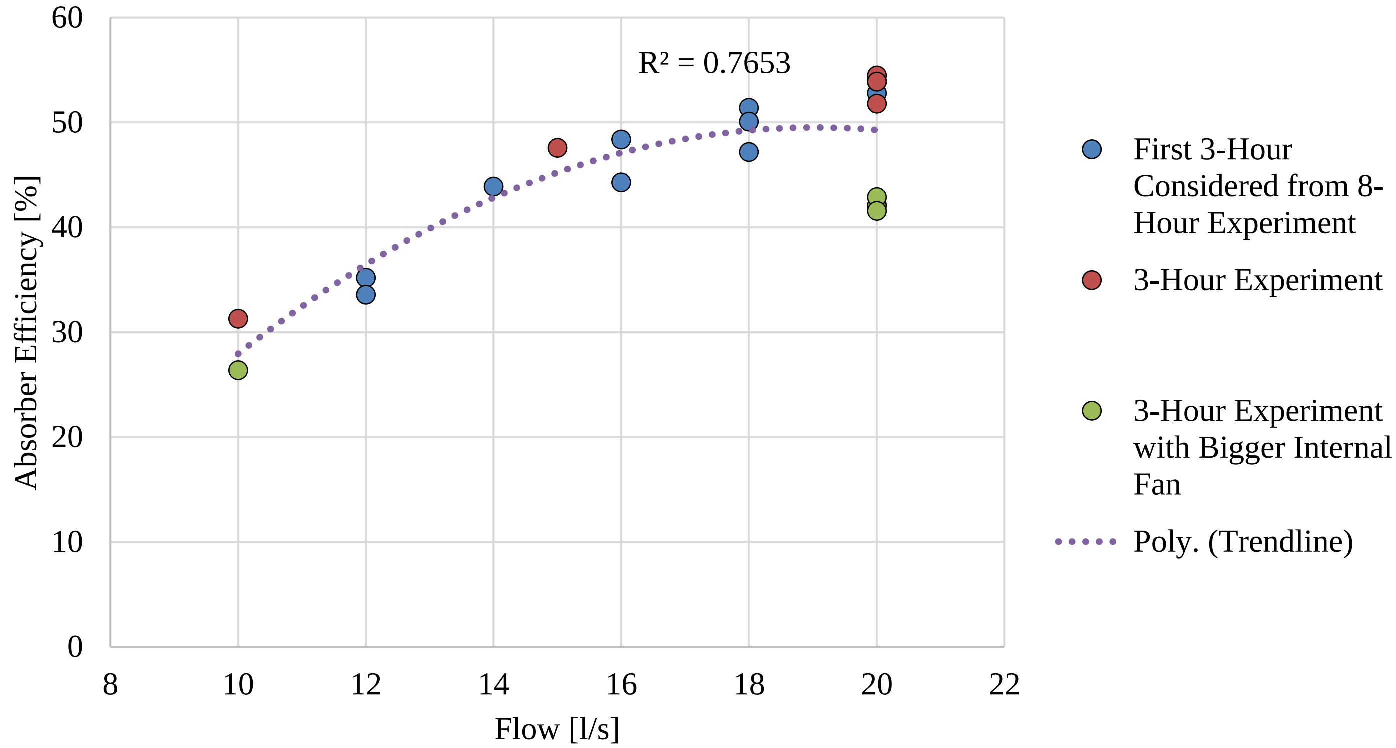

Figure 5-5: The efficiency of the absorber plotted against the flow. The efficiency increases with the increase in the flow.

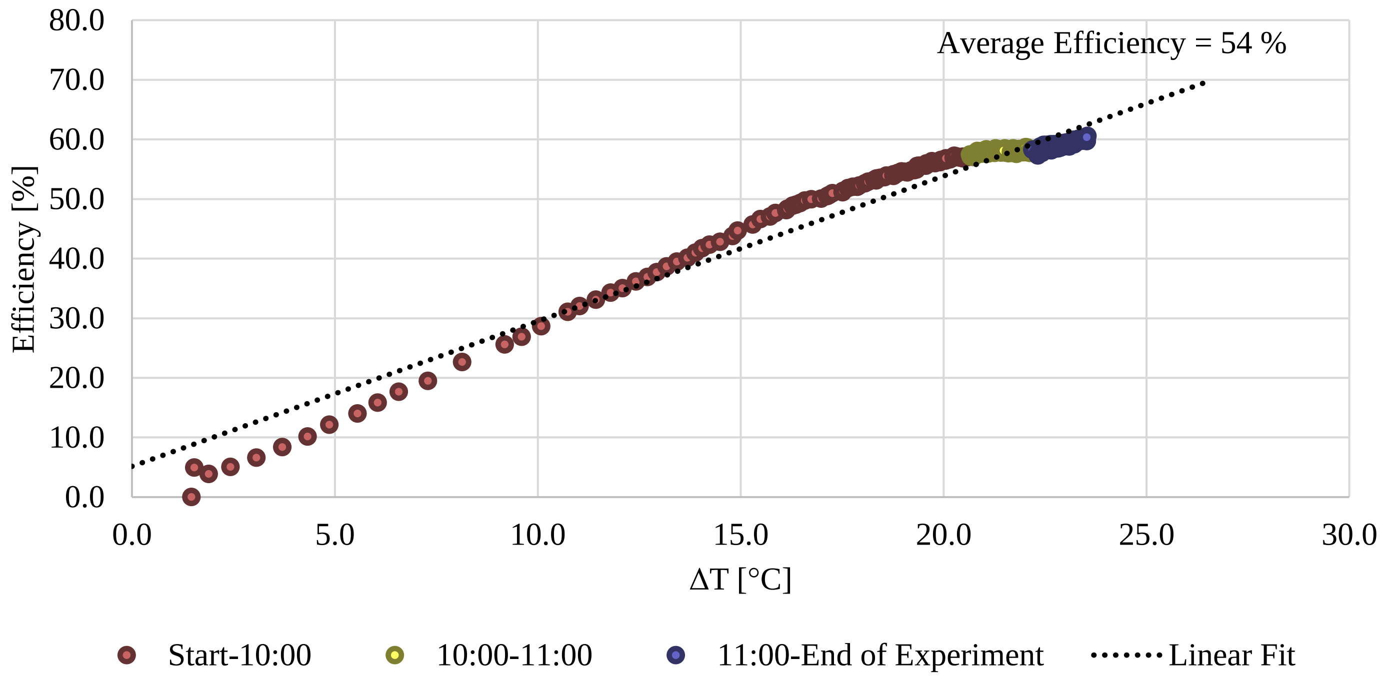

Figure 5-6: The absorber efficiency plotted against the temperature difference between the absorber and the ambient on 23rd May with a flow of 20 l/s. The data points were categorized into three periods of the experiment: first one-third (red), second one-third (yellow), and the remaining time (blue).

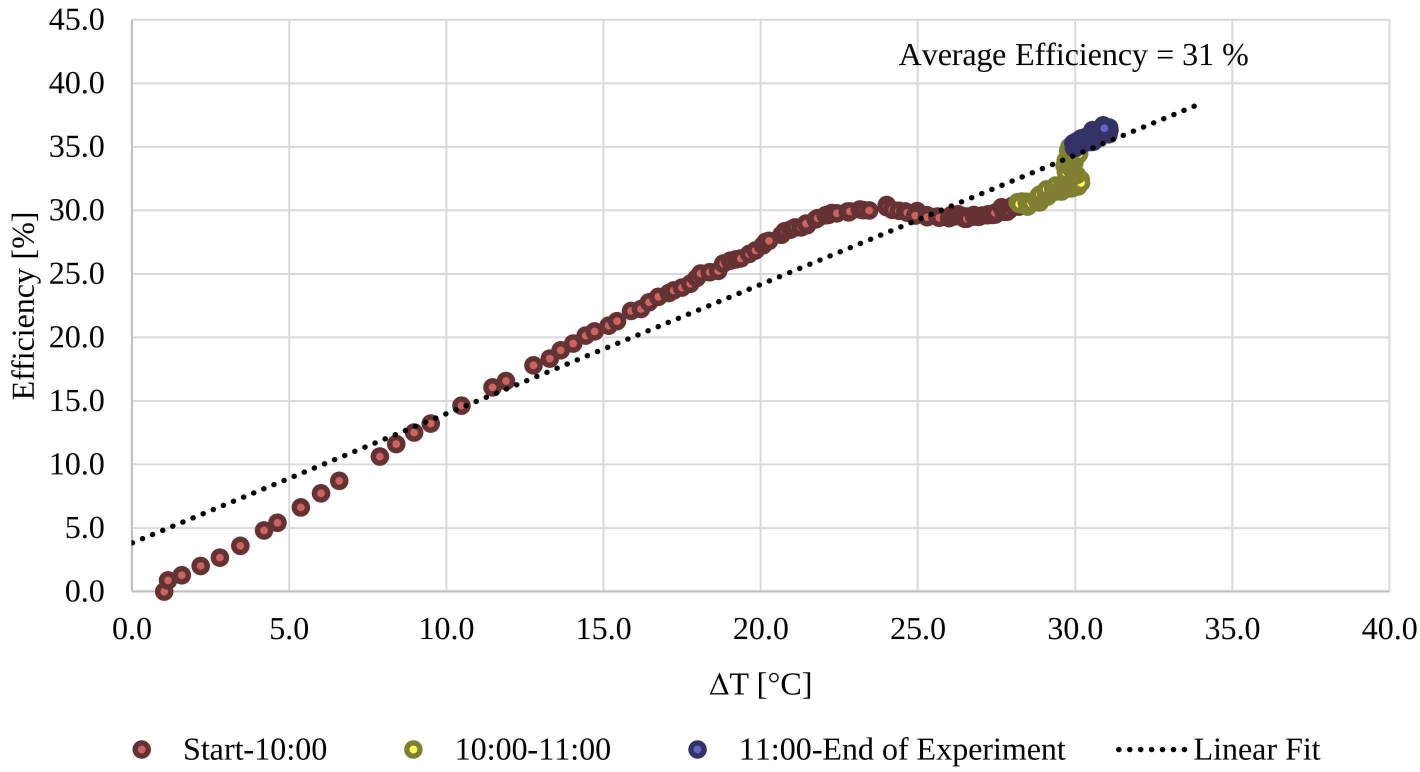

Figure 5-7: The absorber efficiency plotted against the temperature difference between the absorber and the ambient on 24th May with a flow of 10 l/s. The data points were categorized into three periods of the experiment: first one-third (red), second one-third (yellow), and the remaining time (blue).

As shown in *Figure 5-6* and *Figure 5-7*, the efficiency of the absorber increases with the temperature gap between the absorber and the surrounding environment. The efficiency saw a significant boost in the first hour of the experiment due to a substantial temperature difference created. However, the changes in efficiency are less noticeable during the second and third hours. *Figure 5-8* illustrates a continuous increase in absorber efficiency during the initial hour, followed by a nearly stable trend after the commencement of the second hour in the experiment.

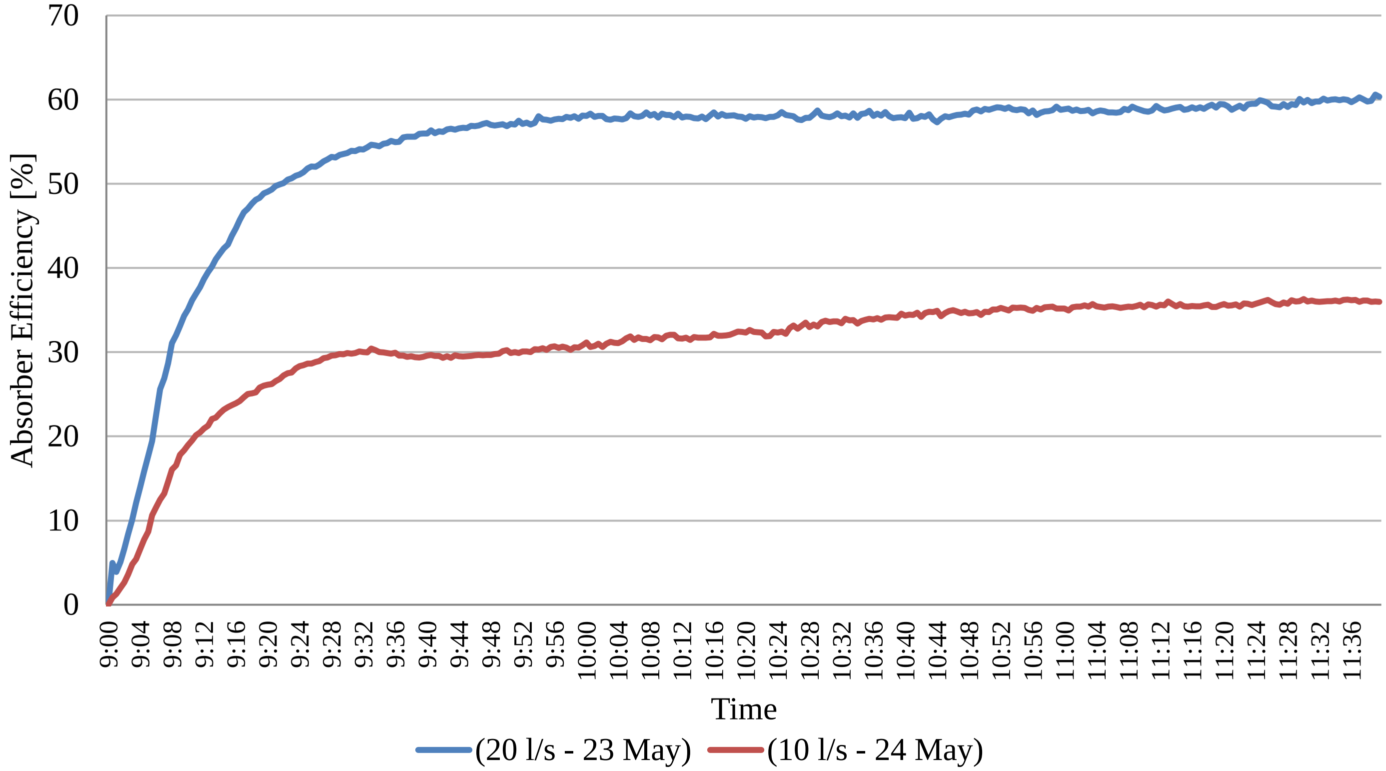

Figure 5-8: The absorber efficiency of 20 l/s and 10 l/s plotted together against the drying time.

5.2.3. Heat storage

In *Figure 5-9* and *Figure 5-10*, the heat flux from heat storage is plotted against time for 20 l/s and 10 l/s respectively.

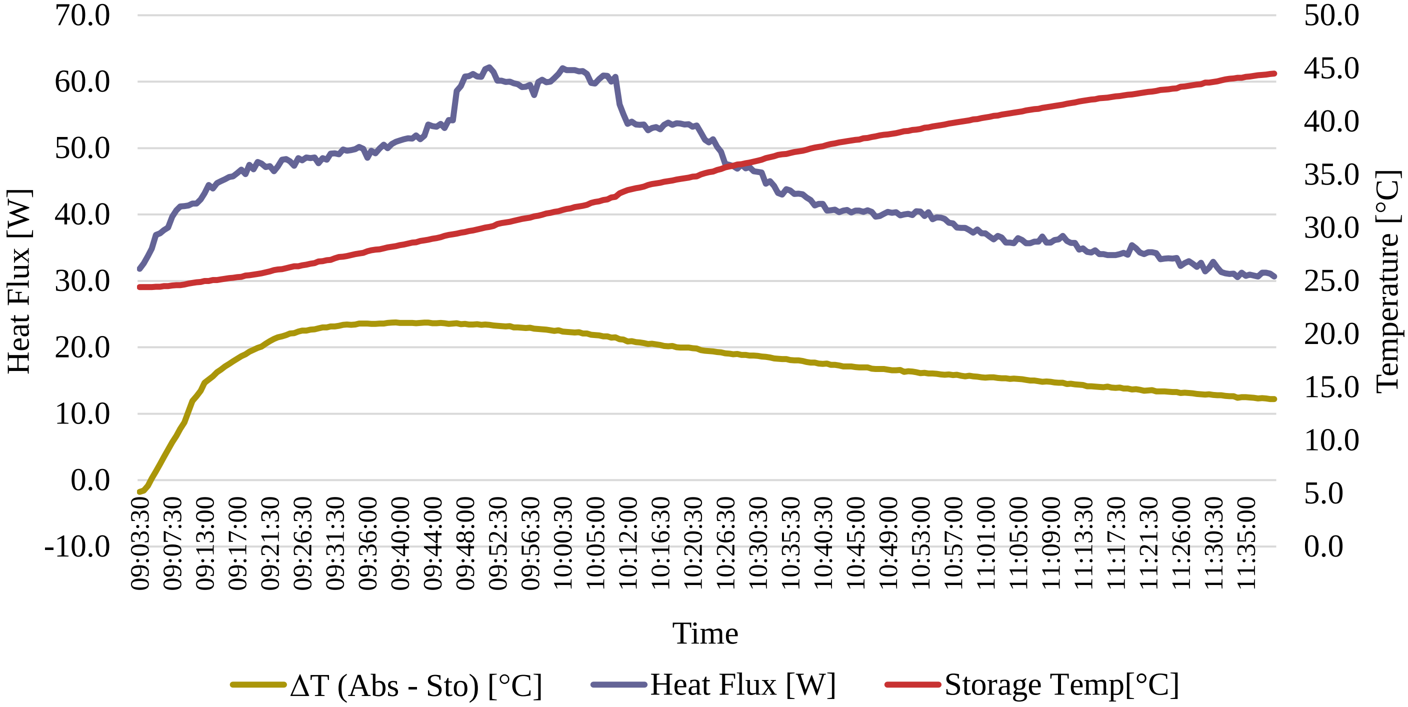

Figure 5-9: The heat flux of heat storage plotted with time along with storage temperature of 20 l/s. The yellow line shows the difference between absorber and storage temperature.

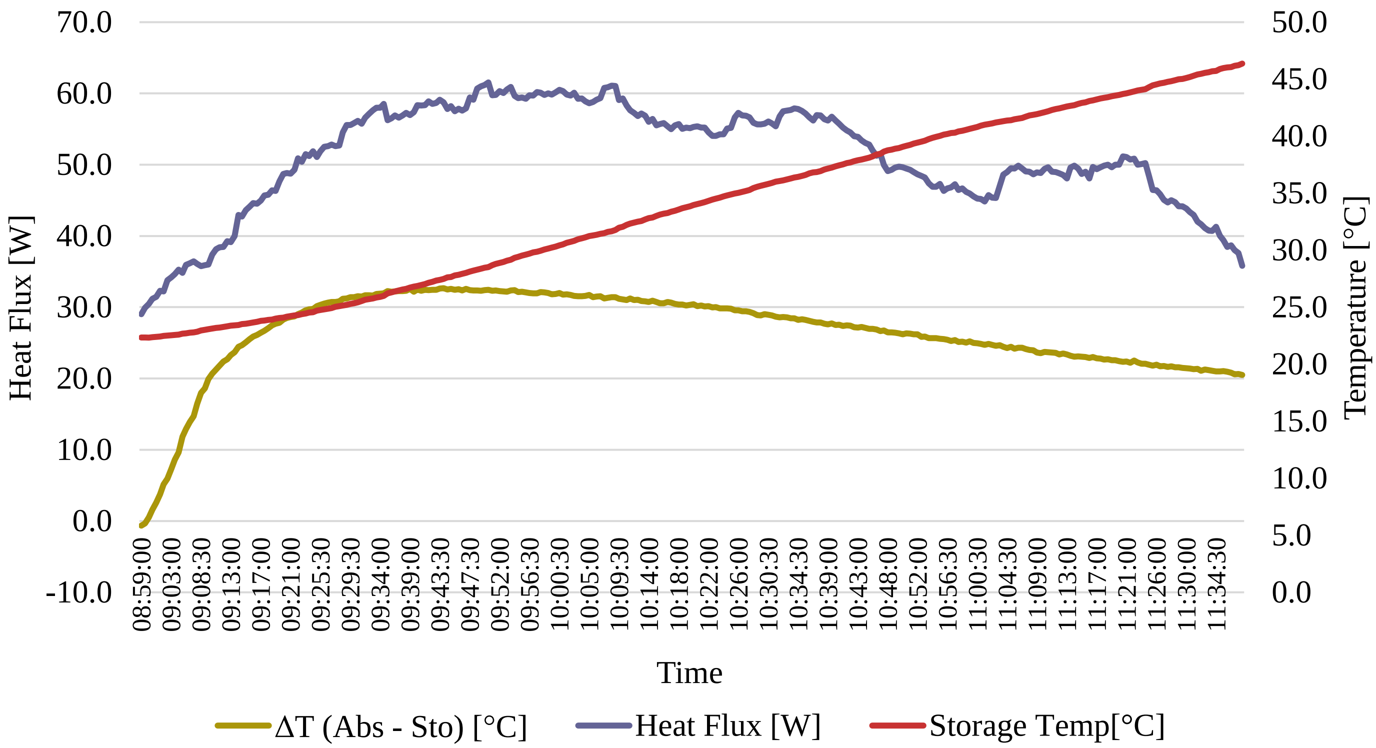

Figure 5-10: The heat flux of heat storage plotted with time along with storage temperature for flow 10 l/s. The yellow line shows the difference between absorber and storage temperature.

Based on the two figures presented above, the heat storage in the solar dryer releases heat to the drying chamber sometime after the start of the experiment. This indicates that the temperature difference between the absorber and the storage diminishes, and as the storage temperature increases, it transfers heat to the drying chamber. The temperature of the heat storage continues to rise steadily throughout the experiment and is anticipated to further increase if the experiment is continued.

5.2.4. Drying chamber

In *Figure 5-11*, the difference between chamber temperature and ambient temperature is plotted against the difference between absorber temperature and chamber temperature for the three-hour experiment duration.

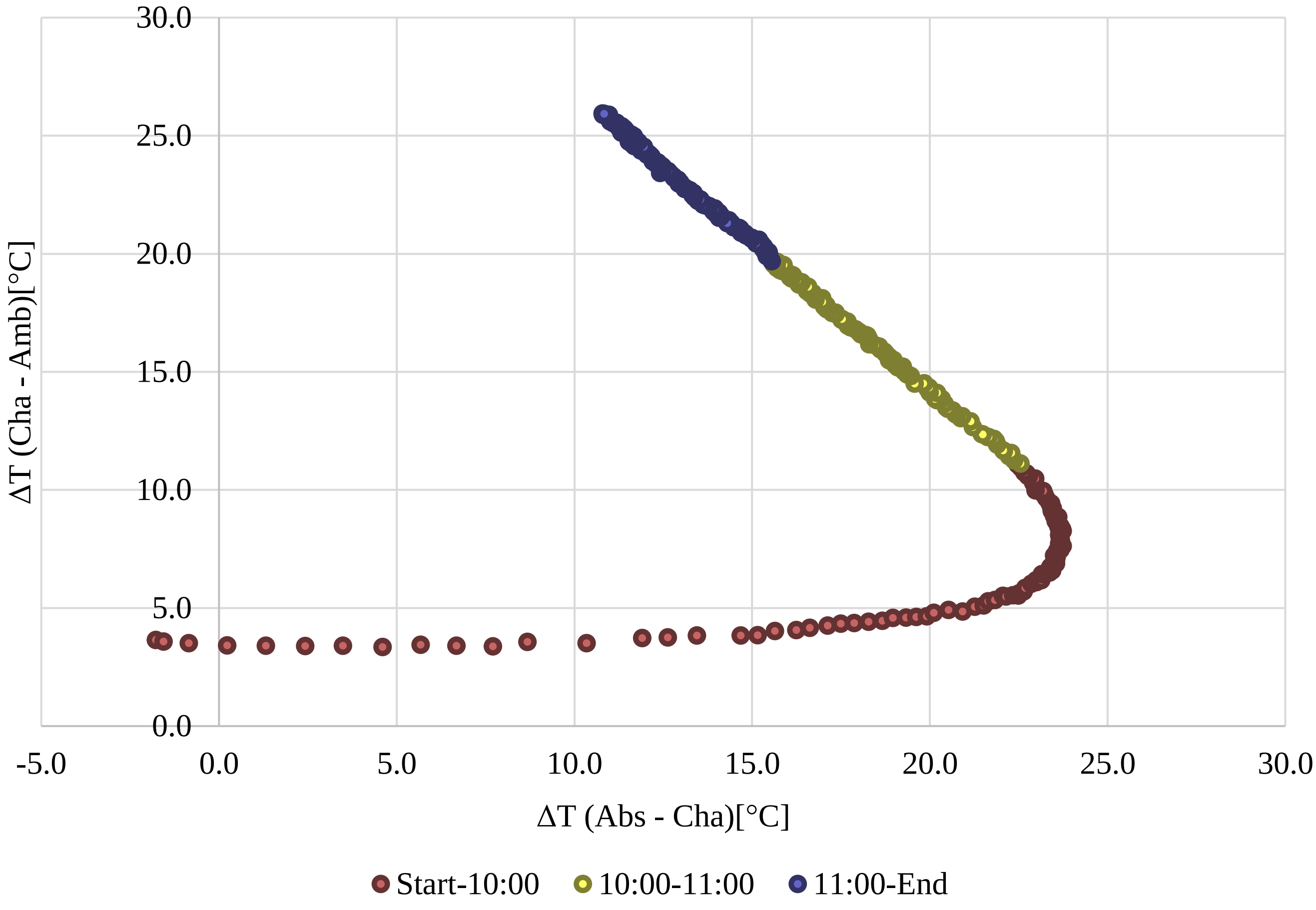

Figure 5-11: The Y-axis represents the variance between the drying chamber temperature and the ambient temperature, while the X-axis represents the disparity between the temperature of the air leaving the absorber and the temperature inside the chamber.

In the initial hour of the experiment, the temperature gap between the absorber and the chamber sharply rises. Simultaneously, the temperature difference between the chamber and the surrounding air remains consistent, except for the latter portion of the first hour. In the second and third hours, the chamber warms up due to the incoming heated air from the absorber, thereby decreasing the temperature difference between the absorber and the chamber. As the chamber temperature rises, the difference between the chamber temperature and the surrounding air temperature widens.

5.2.5. Relative humidity

The relative humidity inside the dryer is a critical factor that significantly influences the drying rate. When the airflow within the dryer is higher, it results in a higher rate of moisture removal from the drying chamber. This is because increased airflow promotes better evaporation and facilitates the movement of moisture-laden air out of the chamber.

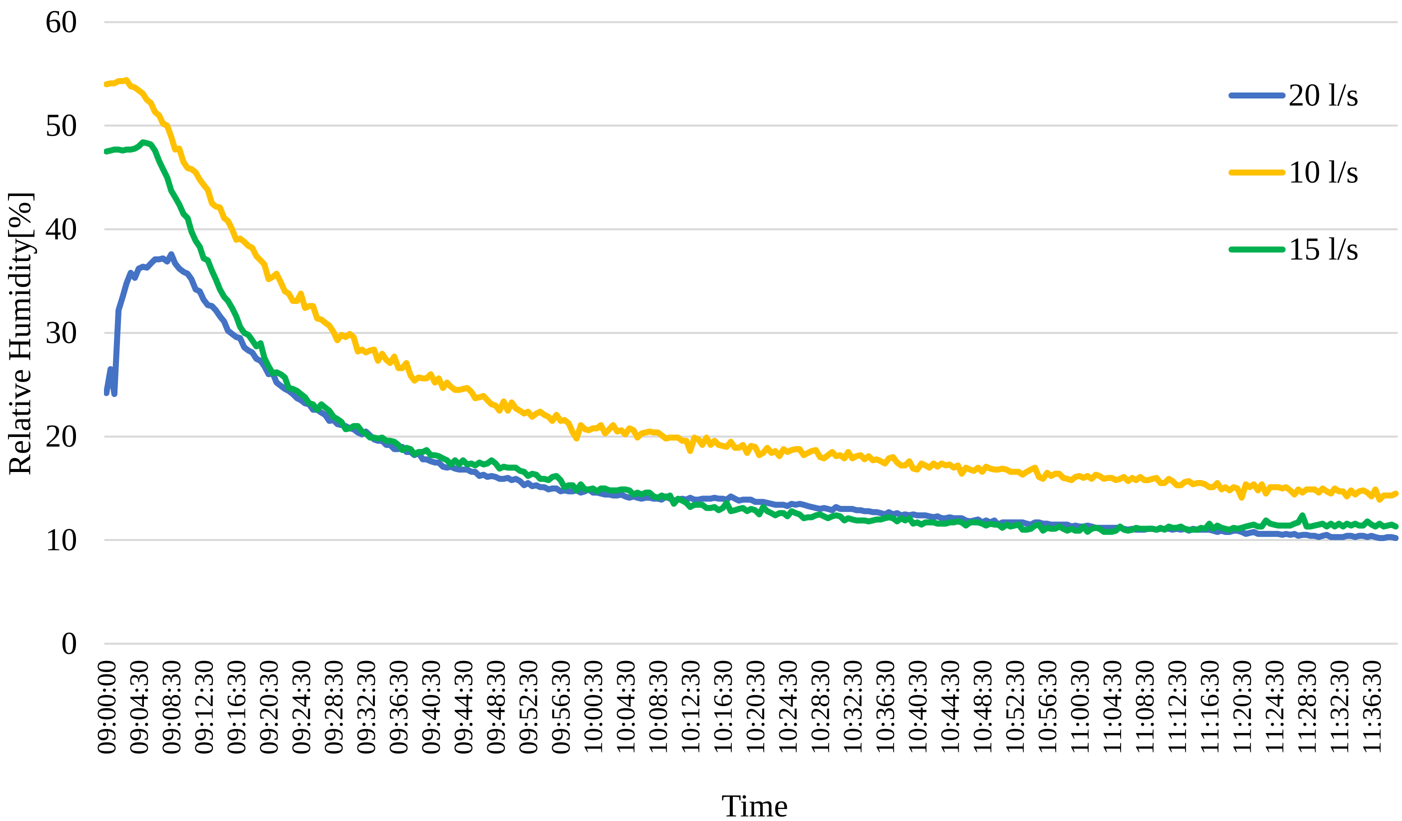

Figure 5-12: The relative humidity plotted with drying time for different flows.

In the case of a higher airflow, such as 20 l/s, the relative humidity inside the dryer decreases more rapidly compared to a lower airflow of 10 l/s as shown in *Figure 5-12*. With a higher flow, the air inside the chamber is replaced more frequently, allowing for faster removal of moisture. As a result, the drying process becomes more efficient, and the moisture content of the drying material decreases at a quicker pace.

On the other hand, when a lower airflow is used, the relative humidity inside the dryer decreases at a slower rate. This means that the moisture removal process is comparatively slower, and it takes more time to achieve the desired level of drying. The lower airflow restricts the exchange of moist air with drier air, leading to a prolonged drying time.

5.3. Individual experiments

In the upcoming sections, the outcomes of the individual experimental setups are examined about the control experiment setup.

5.3.1. Control experiment

In initial experiments, an airflow of 20 l/s achieved optimal drying in 8 hours. Weight measurements at the end suggested faster drying. Hourly measurements in subsequent experiments revealed rapid drying for 3 hours, stabilizing around the 5th hour as shown in *Figure 5-13*.

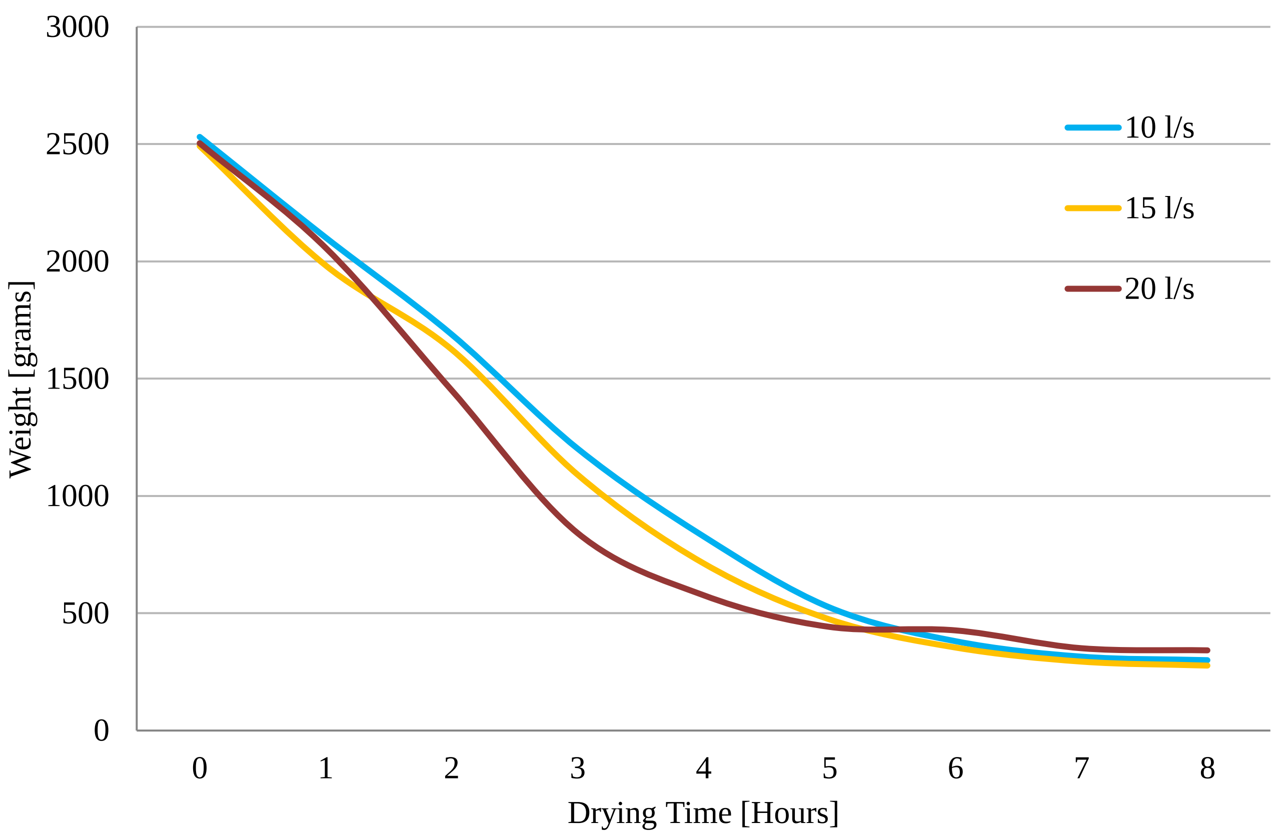

Figure 5-13: The weight of the apple sample plotted against drying time for three flows. It shows the uniformity of the drying rate until 3 hours into the experiment.

To evaluate the drying rate, the weight of each tray was measured per hour using a 20 l/s airflow, which resulted in an overall improved drying rate. The objective was to determine if the apples had sufficiently dried within a 3-hour timeframe.

Figure 5-14 illustrates the findings, indicating that the tray closest to the absorber outlet and positioned in front of the internal fan exhibited the fastest drying rate. This rapid drying trend continued until the 4th hour of the drying process. Conversely, the drying rate of the other trays was slightly slower during the first 2 hours compared to the optimal trays. However, by the 3rd hour, their drying rate aligned with the optimal trays. Subsequently, the drying rate diminished after the 3rd hour. Notably, the drying rate remained relatively consistent until the 4th hour. Based on these observations, it was decided to conduct further experiments with a duration of 3 hours to investigate the drying process with changes to the dryer more comprehensively.

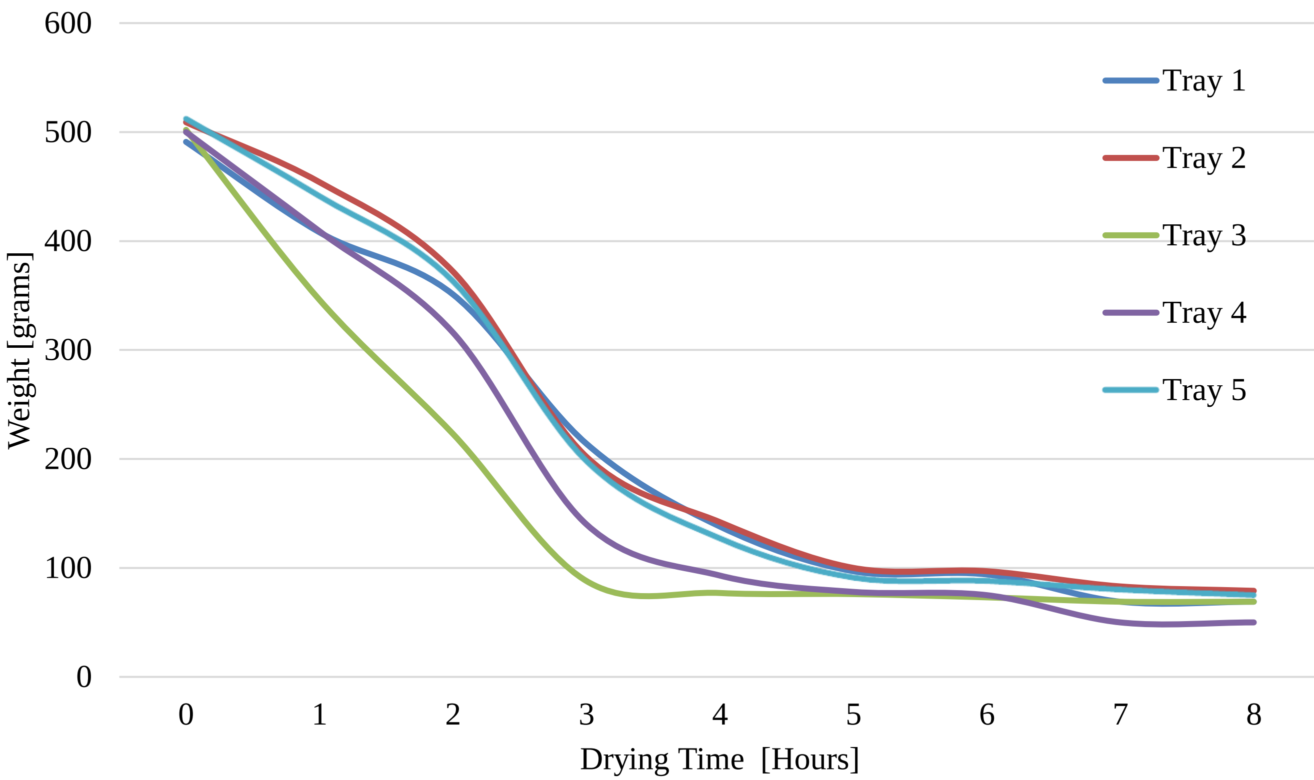

Figure 5-14: The weight per tray plotted against drying time for 20 l/s flow. The linearity of almost all the trays can be seen till the 3rd hour of the drying time.

The data depicted in *Figure 5-14* distinctly illustrates the variances in drying rates between trays positioned optimally within the dryer and those situated at the end of the airflow. The findings emphasize that trays placed closer to the entrance of the airflow from the absorber exhibit higher drying rates, in contrast to trays located at the end of the air circulation within the dryer. This discrepancy underscores the critical importance of tray placement in influencing the efficiency and effectiveness of the drying process. Further insights into these drying rate disparities, along with the inclusion of all the variables made to the dryer, can be found in *Section 5.3.5* of the report, where a detailed analysis of the results is provided.

5.3.2. Open air drying

During the initial two hours of the drying process, both the open-sun and open-shade dried apples exhibited similar rates of weight loss. However, a notable divergence occurred afterwards, as the open sun drying method experienced a rapid increase in weight loss until the third hour, after which it decelerated and mirrored the drying trend observed in the dryers. The results, as depicted in *Figure 5-15*, clearly demonstrate that even after 8 hours of drying, the open sun-dried apples retained a significantly higher moisture content compared to those dried in the dryers. This disparity in moisture content suggests that the open sun drying method may result in apples with higher water activity as compared to apples dried using the dryer.

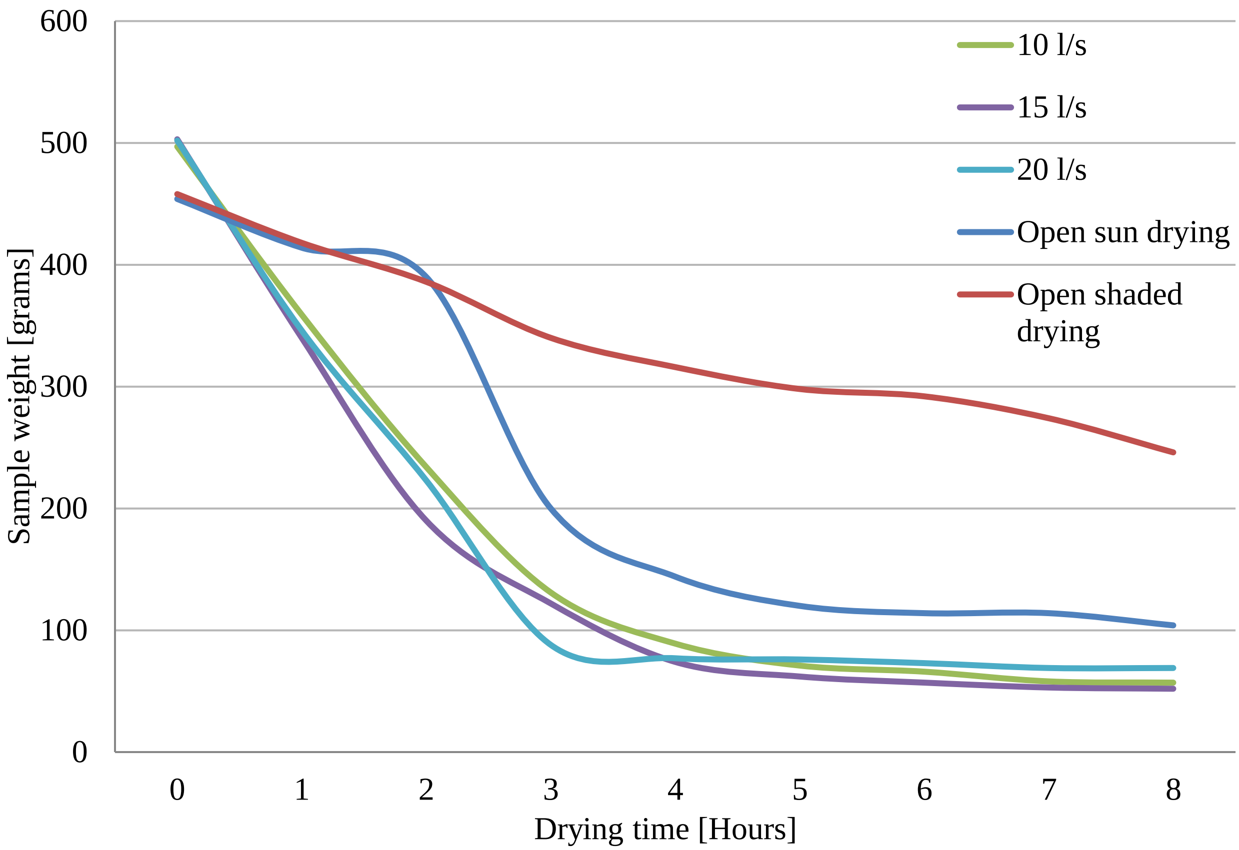

Figure 5-15: The weight of the open sun and open shaded drying as compared to the weight of the apples dried using flow 20 l/s, 15 l/s and 10 l/s (average of all trays for comparison purpose). Note that the open sun and open shade drying was not exposed to any wind or external conditions as a real scenario would be, it was done in a laboratory.

5.3.3. Three hours drying with a bigger internal fan

Figure 5-16 shows the drying rate comparison when the small and big internal fan is used in the dryer. The introduction of a bigger internal fan in the solar dryer led to a significant increase in the drying rate. When compared to the use of a smaller internal fan, the drying rate saw a substantial improvement. At a flow of 10 l/s, the drying rate increased by 25 % with the implementation of the bigger internal fan. Similarly, at a flow of 20 l/s, the drying rate experienced a 15 % increase.

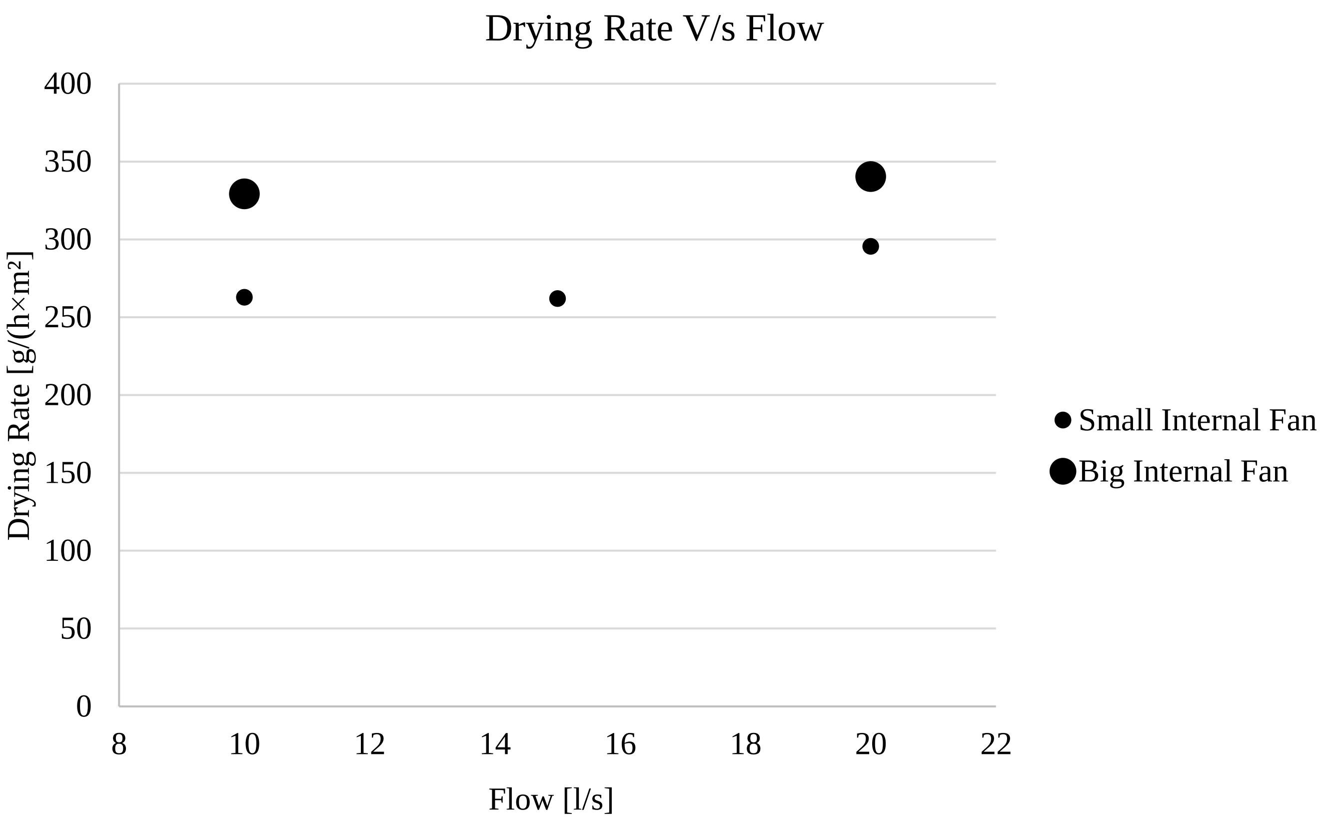

Figure 5-16: The drying rate difference when the smaller internal fan was replaced by a bigger one.

The enhanced drying rate can be attributed to several factors associated with the bigger internal fan. Firstly, the increased airflow generated by the larger fan facilitates better moisture removal from the drying chamber. The greater volume of air being circulated enhances the evaporation process, effectively reducing the drying time. Additionally, the stronger airflow created by the bigger internal fan promotes better air circulation within the drying chamber. As a result, the drying process becomes more efficient, leading to an overall increase in the drying rate.

The improved drying rate observed at both the 10 l/s and 20 l/s flows highlights the effectiveness of the bigger internal fan in enhancing the drying performance of the solar dryer. By increasing the airflow and optimizing air circulation, the bigger internal fan contributes to accelerated moisture removal, resulting in faster drying times.

5.3.4. Drying without heat storage

In *Figure 5-17*, the drying rate is plotted against the drying time for the flow of 20 l/s with the heat storage shown by the blue trendline and without the heat storage by the red trendline.

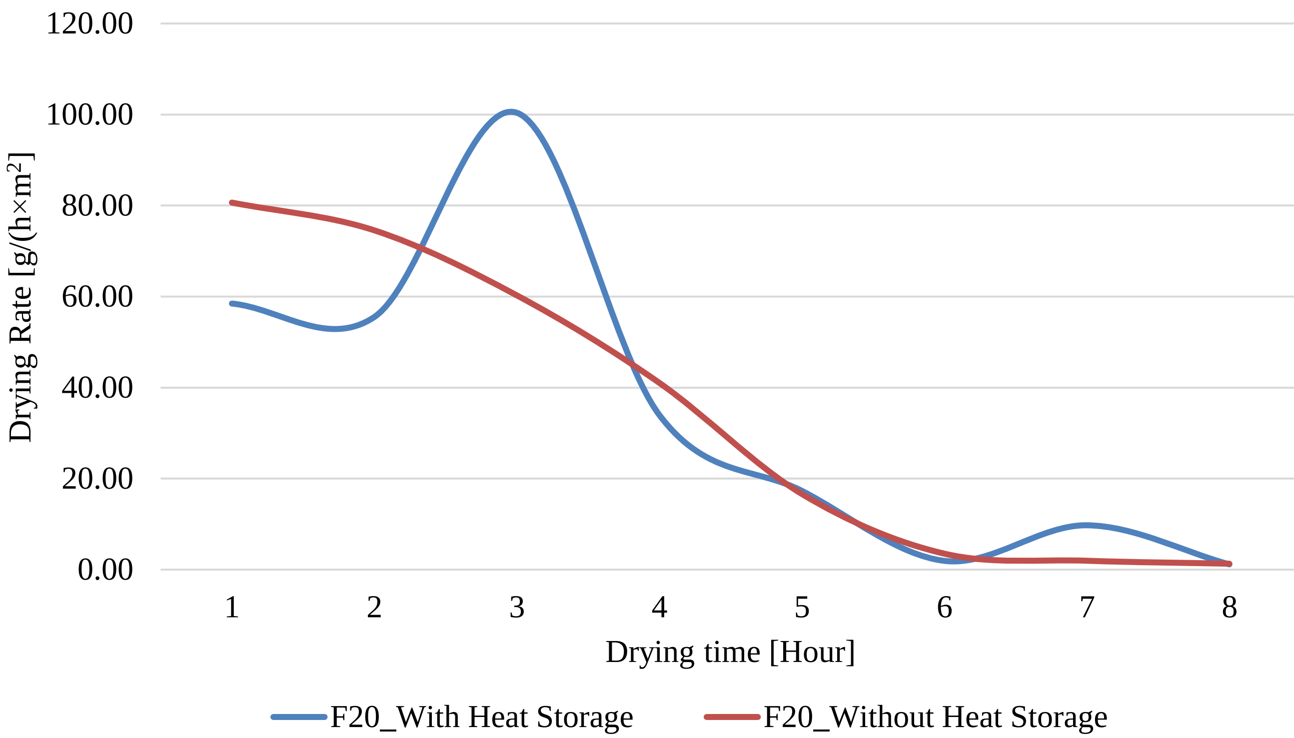

Figure 5-17: The drying rate of 20 l/s in two scenarios with and without heat storage.

During the initial three hours of the drying time experiment, the presence of thermal storage inside the solar dryer did not serve any purpose due to the use of a solar lamp that provided consistent solar irradiation. Without heat storage, the drying rate initially appeared to be higher compared to the setup with heat storage. However, a significant change occurred after the second hour of drying, where the drying rate for the setup with heat storage increased dramatically.

Despite the difference observed during the early stages, the drying rates with and without heat storage converged after three hours of drying. At this point, both setups exhibited similar drying rates, approximately 71.45 g/(hr.m²) and 71.82 g/(hr.m²) for setups with and without heat storage, respectively.

These results suggest that while the presence of thermal storage did not yield a noticeable advantage in the initial hours of drying when solar irradiation was stable, it became more influential as the drying process progressed. The sudden increase in drying rate after the second hour for the setup with heat storage indicates the efficient utilization of stored heat, resulting in improved moisture removal.

However, it is worth noting that beyond the three-hour mark, the drying rates for both setups became comparable, implying that the impact of heat storage on drying efficiency might diminish over extended drying periods. Further investigation like putting off the solar lamps after the 3 hours to see the heat flux and drying rate difference would strongly prove the above results.

5.3.5. Drying rate disparities between best and least drying trays with different setups

Figure 5-18 displays the drying rate difference between the tray with the highest drying rate and the tray with the lowest drying rate. It is evident that as the number of trays used for drying inside the dryer increases, the drying rate decreases. This can be attributed to the fact that with more apple samples to be dried, the same amount of energy and air circulation is spread across a larger surface area, resulting in a slower drying process.

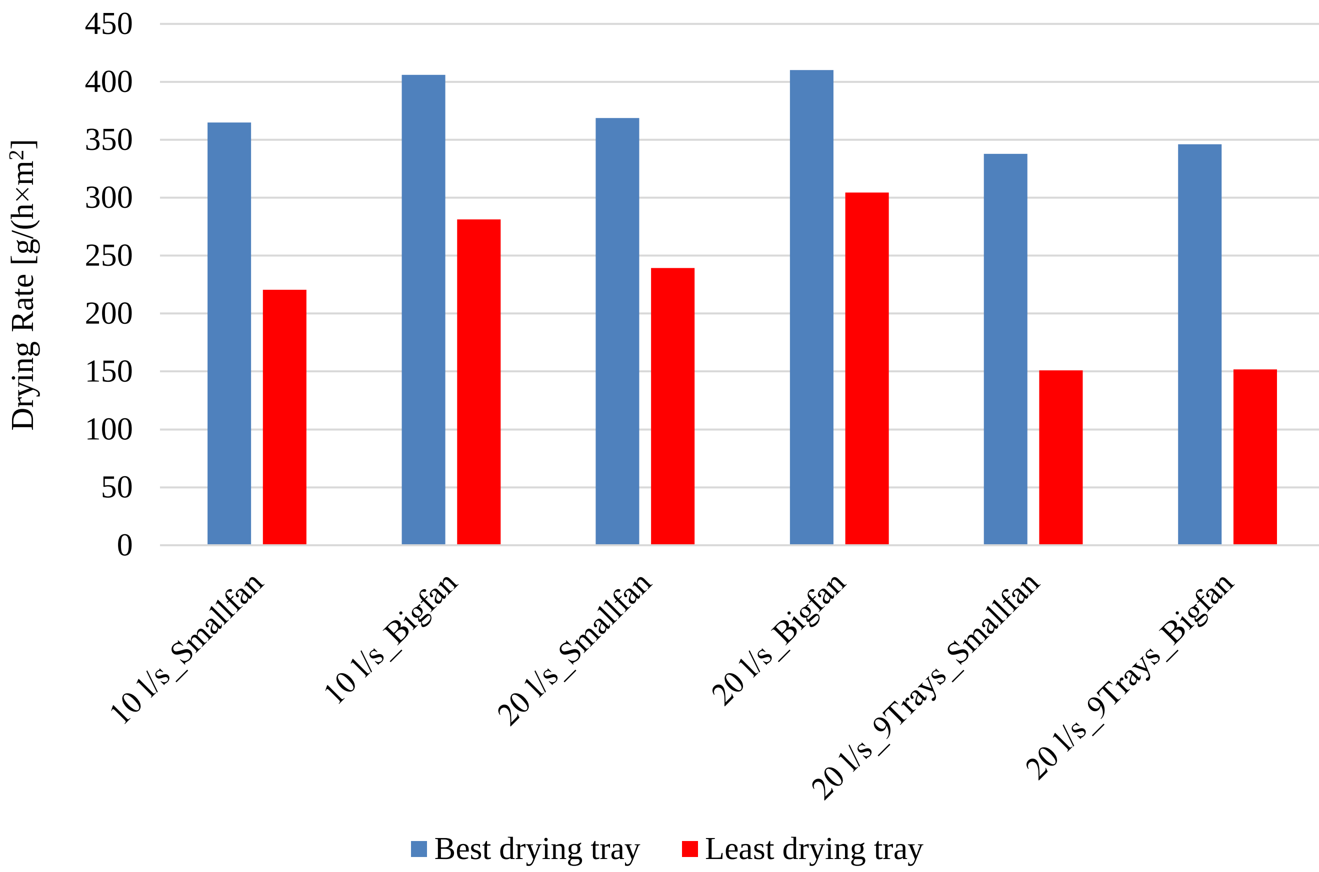

Figure 5-18: Drying rate of different experimental set-ups comparing best and least drying trays.

Furthermore, the difference between the drying rates of the best and least drying trays becomes more pronounced when a small internal fan is employed instead of a bigger internal fan. In other words, when a bigger internal fan is utilized, the disparity in drying rates between the best and worst drying trays diminishes. Using more trays with the same energy input and air circulation leads to a decrease in the drying per area which leads to longer drying time, while employing a larger internal fan helps to mitigate the disparity in drying rates among the trays. As shown *Table 5-1*, with a flow of 10 l/s, the ratio decreased from 1.65 to 1.44, and with a flow of 20 l/s, the ratio decreased from 1.54 to 1.35. This suggests that the larger internal fan helps to decrease the disparity in drying rates between the best and worst trays, resulting in a more uniform drying process.

Table 5-1: Ratio of drying rate between best and least drying trays with different conditions.

Flow_Internal fan size	**Ratio (Best: Lowest)**
10 l/s_Small fan	1.65
10 l/s_Big fan	1.44
20 l/s_Small fan	1.54
20 l/s_Big fan	1.35
20 l/s_9 Trays_Small fan	2.24
20 l/s_9 Trays_Big fan	2.28

However, an interesting observation was made with 20 l/s flow and 9 trays. In this configuration, the ratio of the drying rate between the best and worst trays increased by a small margin. This can be attributed to the specific placement of the additional trays. When the 4 extra trays were added, one of them was positioned directly above the initially best tray, which is located just below the absorber outlet and directly opposite the internal fan. This positioning caused a different trend as compared to the above two cases between the best and worst tray i.e. a slight increase in the drying rate ratio

These findings highlight the importance of considering not only the size of the internal fan but also the arrangement and positioning of the trays within the solar dryer. While a larger internal fan generally helps to reduce the disparity in drying rates, the specific placement of trays can have a significant impact on the drying rate ratio.

6. Discussion

6.1. Drying rate

The study found that higher flows, particularly those generated by a powerful external fan, resulted in the most effective drying rates. Increasing the flow from the fan improved the drying rates, but the experiment couldn't utilize the maximum flow due to the limited voltage rating of the fan. To enhance future studies, it is recommended to use a fan with a higher voltage rating, which is likely to yield better drying results.

Additionally, the size and position of the internal fan within the drying chamber influenced the drying rate. Using a larger internal fan and placing it in the optimal position can contribute to improved drying rates. Exploring the possibility of increasing the number of internal fans within the chamber may also enhance the drying process.

The number of drying trays within the drying chamber was found to impact the drying rate. A higher number of trays resulted in a decrease in the drying rate, while a lesser number of trays led to increased drying rates. For practical applications, it is advisable to increase the number of trays in the chamber while ensuring an increased distance between the trays to facilitate better air circulation.

In calculating the drying rate, the report did not consider the curved surface area of the apple samples due to the limited evaporative capability of the hard apple peel and the significant variation in the radius of the apple slices. The estimation of surface area used in the report was deemed sufficient for the study.

Furthermore, it was observed that the slice surface facing upward dried faster compared to the one facing downward due to the unidirectional internal air circulation. To address this issue, it is suggested to design the internal airflow with a balanced flow in both directions, such as periodically changing the polarity of the internal fan. This approach would likely improve the drying process and result in more uniform drying rates.

6.2. Low-density polyethene as a heat exchanger

A notable distinction in this dryer design is the utilization of low-density polyethene (plastic) as the material for the heat exchanger. Unlike the absorber, the efficiency of the heat exchanger exhibits an inverse relationship with flows. Higher flows were found to result in decreased efficiency, while lower flows yielded increased efficiency. Specifically, at a flow of 20 l/s, the heat exchanger's efficiency was approximately 50 %, whereas at a flow of 10 l/s, the efficiency increased to approximately 67 %.

Remarkably, the experiment revealed that the polyethene sheet performed remarkably well as a heat exchanger, achieving an efficiency level of around 60 %. This finding underscores the potential advantages of incorporating plastic heat exchangers. In comparison to metal sheets, plastics are significantly more cost-effective, making them a favourable choice for practical applications. Additionally, the use of plastic heat exchangers offers enhanced ease of working with the material, further enhancing their appeal in the context of this solar dryer design.

The successful utilization of low-density polyethene as a heat exchanger material highlights the potential for cost savings and practicality in solar dryer systems. By maximizing the efficiency of the heat exchanger while maintaining a balanced flow, it is possible to achieve optimal performance and energy utilization. The affordability and ease of handling plastic heat exchangers provide a promising avenue for future developments and widespread adoption of solar drying technology.

6.3. Drying chamber

In the context of the experiment, the early hours revealed an interesting trend in the temperature dynamics within the drying chamber. This behaviour can be attributed to the presence of a larger-sized absorber, which facilitated the maintenance of higher temperatures. When a flow of 20 l/s was employed, the temperature within the chamber quickly rose to a peak range of approximately 31 °C to 41 °C. This temperature range coincided with the optimal conditions for achieving desirable drying results.

Furthermore, the number of trays placed inside the drying chamber exerted a notable influence on both the temperature and the drying profile among the different trays. It is important to consider that in real-world scenarios, farmers would typically aim to dry as many different fruits as possible in a single drying cycle. This aspect introduces additional complexities and variables that were not fully captured in the experimental setup. The performance and drying rates of the dryer system would likely differ significantly when subjected to the uncertainties associated with real-world weather conditions.

It is worth noting that the constant solar irradiation provided in the experiment provided a consistent energy source, thus deviating from the variability and unpredictability of weather conditions typically experienced in agricultural settings. Consequently, the findings presented in this report might not fully reflect the performance and drying outcomes that would be encountered in practical applications. In real-world scenarios, farmers would need to consider the uncertainties of weather patterns and their impact on drying rates, which could potentially introduce additional challenges and variations to the drying process.

6.4. Tradeoff between better absorber and heat exchanger

The study revealed an interesting idea of a trade-off between the absorber and the heat exchanger in terms of efficiency and chamber temperature. The absorber demonstrated its highest efficiency with the highest flow, while the heat exchanger achieved its highest efficiency with the lowest flow. Surprisingly, both setups resulted in similar chamber temperatures of approximately 35.6 °C and 36 °C.

To determine the optimal setup, a balance needs to be found between the absorber and the heat exchanger, considering their respective efficiencies and chamber temperatures. In the current setup, since the heat exchanger is made of plastics, economic considerations might lean towards focusing more on the absorber. However, real-world scenarios with irregular solar insolation introduce additional complexities. This raises the question of how much importance should be given to the absorber or the heat exchanger in achieving the desired performance and efficiency.

Further experimentation and analysis are necessary to explore the trade-offs and find the optimal configuration that maximizes overall system efficiency while considering the cost-effectiveness of the materials used. Factors such as varying solar insolation patterns, environmental conditions, and long-term performance need to be considered to determine the ideal balance between the absorber and the heat exchanger in solar drying systems. This will help in designing systems that are not only efficient but also economically viable and well-suited to real-world operating conditions.

6.5. Internal fan

The effectiveness of the drying process in the solar dryer was significantly influenced by the choice of an internal fan. The use of a better internal fan provided a clearer basis for comparison among different experiments. It improved the accuracy of drying rate measurements and facilitated a more precise evaluation of the drying conditions. The enhanced airflow generated by the improved internal fan contributed to better heat and moisture transfer, resulting in more consistent drying rates.

Moreover, the inclusion of a better internal fan led to improved control over the chamber temperature. The enhanced airflow circulation within the drying chamber minimized temperature disparities among the different trays, ensuring more uniform drying conditions. This not only improved the reliability and predictability of the drying process but also increased its overall efficiency.

However, the introduction of more internal fans into the system requires careful consideration due to the associated costs. While additional internal fans would likely yield further improvements in drying rates and temperature control, they would also increase the overall cost of the dryer. Therefore, a thorough cost-benefit analysis is essential to evaluate the trade-off between the benefits gained from incorporating extra accessories and the financial implications involved.

Further research and in-depth cost-benefit analysis are necessary to determine the ideal number of internal fans and assess their impact on the overall performance and cost-effectiveness of the solar dryer system. This analysis will enable us to make informed decisions about the inclusion of extra internal fans, considering both the potential advantages they offer and the financial viability of the improved system.

6.6. Thermal storage

In the initial stage of the drying process, the presence of heat storage in the dryer system leads to heat absorption from the surrounding environment, resulting in a temporary decrease in the drying rate. However, as the heat storage accumulates the necessary amount of heat, it plays a crucial role in maintaining and regulating the temperature within the drying chamber. Additionally, the heat loss experienced during the initial heating phase can be compensated for towards the later stages of the drying process when there is no available solar radiation to further increase the air temperature. On the other hand, in a setup without heat storage, the drying rate initially increases rapidly but gradually diminishes over time. Interestingly, both setups, with and without heat storage, demonstrated similar drying rates of approximately 71.45 g/(hr.m^2) and 71.82 g/(hr.m^2) respectively. This suggests that the inclusion of thermal storage for short-duration drying, under conditions of consistent solar irradiation, does not significantly impact the overall performance of the dryer.

It is important to note that the aforementioned drying rates were obtained over a relatively short drying period of 3 hours, assuming a constant supply of solar radiation. In practical scenarios where, solar insolation fluctuates and larger quantities of fruits or vegetables need to be dried, the use of heat storage could prove to be beneficial. The variability in solar radiation and the need to process substantial amounts of produce would introduce additional complexities and challenges beyond the scope of this experimental study. Therefore, it is plausible that heat storage could play a vital role in enhancing the performance and efficiency of the dryer, ensuring consistent drying outcomes in real-world applications.

7. Conclusion

This study investigated the performance of an indirect-type solar dryer and provided valuable insights into its drying efficiency and effectiveness. The findings revealed that higher flows resulted in improved drying efficiency, leading to more homogeneous drying conditions across the different trays. However, the introduction of more trays in the drying chamber increased drying disparities, indicating a decrease in the overall efficiency of the dryer. Nevertheless, this discrepancy can be mitigated by enhancing the internal flow through the utilization of a greater number of internal fans, larger-sized internal fans, or by implementing a better design for air circulation inside the dryer.

Another significant outcome of this research pertains to the utilization of low-density polyethene, a cost-effective material with a thickness of 0.2 mm and a low thermal conductivity of 0.331 W/m K, as an efficient heat exchanger. The experimental results demonstrated that the low-density polyethene sheets performed exceptionally well, proving to be a suitable alternative to more expensive metal sheets.

In summary, the optimal configuration for the solar dryer under investigation involved the incorporation of a better internal fan with an improved airflow design, employing the highest achievable flow. Furthermore, the inclusion of a heat storage component facilitated better heat distribution over time, resulting in superior drying outcomes. This study contributes to the understanding of solar drying systems and highlights the potential of optimizing drying efficiency through careful consideration of factors such as internal fan selection, airflow design, and the choice of heat exchanger material. The findings underscore the importance of these design aspects for achieving efficient and effective drying in the current solar dryer setup.

8. Limitations of the study and Recommendations

The experimental setup in this study was conducted in a controlled laboratory environment, which may not fully capture the complexity of real-world conditions. The use of constant solar irradiation and the absence of environmental factors such as wind and outside relative humidity could have limited the applicability of the findings to practical scenarios. These factors play a significant role in determining the performance of solar dryers, and their exclusion from the experiment might have influenced the results. Additionally, the placement of thermocouple sensors at the outlet of the dryer was shifted to the side of each third of the section due to plastic heating and contact issues, potentially introducing measurement errors and affecting the accuracy of the heat exchanger performance assessment. To mitigate these limitations, further research is needed to validate the findings in more realistic settings and address the measurement challenges associated with heat exchanger sensors.

Some of the future recommendations and improvements to be made to the current setups are:

- ➔ Analyze drying rate disparities based on tray positioning in the chamber and explore methods to minimize differences.
- ➔ Optimize the placement of internal fans to prevent air reverse flow into the absorber and improve overall system efficiency.
- ➔ Consider using a better and stronger external fan to determine the peak efficiency of the solar dryer.
- ➔ Investigate alternative materials for the heat exchanger to evaluate their performance compared to the current setup.
- ➔ Simulate solar lamps to provide a more realistic solar irradiation scenario, including variations such as turning off certain lamps during specific times of the day, to better align with real-world conditions and conduct experiments that account for varying solar energy availability.

Both authors collaborated on this study. Tandin Jamtsho designed the solar dryer and wrote Chapters 4 and 5, while Dechen Om worked on Chapters 1, 2, and 3. The remaining chapters (6, 7, and 8) and the experiments were a joint effort by both authors.

References and Bibliography

Bala, B. K., & Woods, J. L. (1994). Simulation of the indirect natural convection solar drying of rough rice. *Solar Energy*, *53*(3), 259–266. https://doi.org/10.1016/0038-092X(94)90632-7

Brown, A., & Johnson, C. (2019). Nutritional value of dried fruits. In J. Smith (Ed.), *Advances in Food Science and Technology* (pp. 45-62*)*. Springer.

Brown, M., Smith, D., & Wilson, E. (2022). Design and optimization of fruit solar dryers. *Renewable Energy*, *155*, 1123-1134.

Can, A. (2000). Drying kinetics of pumpkin seeds. *International Journal of Energy Research*, *24*(11), 965–975. https://doi.org/10.1002/1099-114X(200009)24:11<965::AID-ER635>3.0.CO;2-W

Chowdhury, F. K., Rahman, M. M., & Saidur, R. (2012). Performance enhancement of solar air heater by using obstacles at different positions. *International Journal of Energy and Environmental Engineering*, *3*(1), 1-9.

Cm, K. (n.d.). *Vejledning til håndpyranometer med display User's Guide : Hand pyranometer with display*.

Elevation of Lund,Floodmap.net. (n.d.). Retrieved June 30, 2023, from https://www.floodmap.net/elevation/ElevationMap/?gi=2693678

Garcia, R., & Thompson, L. (2018). Fruit solar dryers: A sustainable solution for post-harvest preservation. *Journal of Sustainable Agriculture*, *41*(3), 215-230.

Green, S., & Taylor, P. (2021). The economic impact of fruit solar dryers on small-scale farmers. *Agricultural Economics*, *56*(4), 567-583.

Gwala, W., & Padmavati, R. (2015). Comparative study of degradation kinetics of ascorbic acid (vitamin C) in tray drying, solar drying and open sun drying of pineapple slices. *Austin Journal of Nutrition & Metabolism*, *2*(1), 1014–1019. www.austinpublishinggroup.com

Harris, J., Miller, K., & Robinson, S. (2023). The role of fruit solar dryers in reducing post-harvest losses. *Food Security*, *15*(1), 215-230.

Jones, T., Smith, A., Brown, M., & Johnson, K. (2020). Trends in dried fruit consumption over the centuries. *Journal of Historical Food Studies, 7*(2), 123-140.

Jackson, R., & White, L. (2020). Dried fruits: A comprehensive review of health benefits. *Nutrition Reviews, 78(2)*, 77-91.

Kilanko, O., Ilori, T. A., Leramo, R. O., Babalola, P. O., Eluwa, S. E., Onyenma, F. A., Ameh, N. I., Onwordi, P. N., Aworinde, A. K., & Fajobi, M. A. (2019). Design and Performance Evaluation of a Solar Dryer. *Journal of Physics: Conference Series*, *1378*(3). https://doi.org/10.1088/1742-6596/1378/3/032001

Kipp & Zonen. (n.d.). *Pyranometer for outdoor installation. Model CM5 - CM6.* 5–6.

Krittacom, B., Bunchan, S., & Luampon, R. (2022). Heat transfer enhancement of solar collector by placing wire mesh stainless porous material on the solar absorber plate of indirect forced convection solar dryer. *Thermal Science and Engineering Progress*, *32*, 101304.

Kumar, A., Tiwari, G. N., & Kumar, A. (2017). Performance evaluation of a solar dryer with heat exchanger for drying agricultural products. *Journal of Food Science and Technology, 54*(12), 3965–3975.

Kundu B. Performance analysis and optimization of absorber plates of different geometry for a flat plate solar collector: a comparative study. *Applied thermal engineering. 2002 Jun 1;22*(9):999-1012.

Lee, H., & Martinez, E. (2019). Solar collectors for fruit drying: A comparative study. *Solar Energy, 186*, 201-215.

Min, M. A. X., & Max, M. I. N. (n.d.). *CO2/Humidity/Temperature Datalogger, Model SD800.*

Miller, E. (2021). Health implications of dried fruit consumption. *Journal of Nutritional Science, 10,* e45.

Robinson, S. (2017). Dried fruits in modern diets: A review of current research. *International Journal of Food Sciences and Nutrition, 68*(7), 829-841.

Robinson, S., & Smith, D. (2022). Fruit solar dryers in rural communities: A case study in sustainable technology adoption. *Renewable and Sustainable Energy Reviews, 151*, 1215-1230.

Singh, J. (no date) *Review paper of study on Solar Dryer.* Available at: https://core.ac.uk/download/pdf/230489679.pdf (Accessed: 26 June 2023).

Smith, J. (Ed.). (2018). Dried Fruits: Production, Processing, and Nutrition. *Wiley-Blackwell.*

Smith, J., & Wilson, E. (2020). Solar drying of fruits: A comprehensive review. *Journal of Food Engineering, 271*, 109761.

The Engineering Toolbox. 2003. Air - Density, Specific Weight and Thermal Expansion Coefficient vs. Temperature and Pressure. Accessed 05 28, 2023.

Thomas, G. (2022). Culinary applications of dried fruits in modern gastronomy. *International Journal of Gastronomy and Food Science, 26*, 100331.

Wangmo, C., & Dendup, T. (2021). Post-Harvest Handling and Losses of Green Chilies: A Case Study from Bhutan. *Indonesian Journal of Social and Environmental Issues (IJSEI), 2*(3), 284–292. https://doi.org/10.47540/ijsei.v2i3.329

White, L., & Brown, M. (2023). The economic viability of fruit solar dryers for small-scale farmers. *Renewable Agriculture and Food Systems, 38*(2), 193-210.

Yilmaz, M., & Hires, S. E. (2014). Experimental and numerical analysis of heat transfer and fluid flow in an inclined solar air heater. *International Journal of Heat and Mass Transfer, 70*, 355-366.